# EFFECTS OF FORMWORK DIMENSIONS ON THE MECHANICAL PERFORMANCE OF FIBER-REINFORCED CEMENT BASED MATERIALS

by

İrem ŞANAL

B.S., Civil Engineering, Boğaziçi University, 2008

Submitted to the Institute for Graduate Studies in
Science and Engineering in partial fulfillment of
the requirements for the degree of
Master of Science

Graduate Program in Civil Engineering

Boğaziçi University

2010

# ACKNOWLEDGEMENTS

First and foremost I offer my sincerest gratitude to my supervisor, Dr. Nilüfer Özyurt, who has supported me throughout my thesis with her patience and knowledge. Without her, this thesis would not have been completed or written. One simply could not wish for a better and friendlier supervisor.

I would like to express my deepest appreciation to Dr. Osman Börekçi for helping me to develop my scientific background, acquainting me with academic life and showing me the joy of intellectual pursuit.

Its a pleasure to thank Dr. Erhan Karaesmen, for his academic and lifetime supports.

I also thank the members of my graduate committee, Prof. Turan Özturan and Dr. Altuğ Söylev, for their guidance and suggestions. I am thankful that in the midst of all their activity, they accepted to be members of my thesis committee.

I am grateful to Bogazici University Construction Materials Laboratory staff: Ümit Melep and Mesut Kardaş, and Bogazici University Structures Laboratory staff: Hasan Şenel and Hamdi Ayar, who helped me very much during my experiments. I would like to show my gratitude to Bogazici University Research Fund (Project Code 09HA401P), AKCANSA and BASF-YKS for their supports.

I would never be able to thank enough for all of the support my parents, Handan Şanal and Faruk Şanal, who have given to me for the past 23 years of my life. I would like to thank to them for their support, encouragement and especially for the smile that they have never hesitated to show me.

I am heartily thankful to my dear, lovely sister, İstem Şanal, for her accompany throughout my graduate studies. I am very lucky to have such a best friend like her, apart from being the greatest sister forever.

My grandparents, Nimet Söyleyensoy and Ahmet Söyleyensoy, deserve special mention for their endless support and prayers. They were always there cheering me up and stood by me through the good times and bad times. Without their encouragement, I would not have finished this degree.

It is a pleasure to thank to all of my friends, for supporting me in every step I take and motivating me throughout both my undergraduate and graduate studies.

Furthermore, I would like to offer my regards and blessings to everybody who supported me in any respect during the completion of my thesis, as well as expressing my apology that I could not mention personally one by one.

I would like to dedicate my thesis to such an amazing and perfect person, who has a place of honor deep within my heart; my deceased grandfather Ahmet Söyleyensoy, who passed away when I was in the middle of the writing of my thesis**.**

# ABSTRACT

## EFFECTS OF FORMWORK DIMENSIONS ON THE MECHANICAL PERFORMANCE OF FIBER-REINFORCED CEMENT BASED MATERIALS

The aim of this work was to study the relationship between formwork/sample variables and fiber properties to help define design principles of structures, generally when fiber reinforced materials are considered. For this purpose parameters such as formwork dimensions and fiber aspect ratio were varied and related to resulting fiber dispersion state and mechanical performance. Two parameters were defined to understand the effects of varying formwork dimensions on the fiber alignment and resulting mechanical performance. Two different length of the same steel fibers were used. One of the parameters was selected to be the ratio of formwork or flow width to the fiber length (w/fL) and the other one was the ratio of formwork thickness to the fiber length (t/fL). Two concrete mixtures with two different length of the same fiber were cast into formworks with varying thicknesses and widths to obtain various flow behaviors from the materials. Six different w/fL and 4 different t/fL values were obtained and results evaluated by using optical image analysis and mechanical tests.

A series of experiments were performed to correlate the fresh and hardened state properties of FRCs by means of fiber dispersion and orientation. Specimens were cast using same mix designs, only fiber length and specimen depth parameters were varied. Two different mixes were prepared by varying fiber length and two different specimen thickness values were set. Therefore, 4 different groups of specimen were obtained. These FRC's are cast into different size of moulds, having same length and depth, but vario ¡ widths. Before exposing to flexural test, each specimen having various widths were cut in order to make all the specimens have the same width. After that, in order to determine the hardened state properties, specimens were exposed to four-point bending test.

Finally, image analysis were conducted in order to better understand fiber orientation. To do fiber orientation analyses, specimens were cut into 2 pieces, near the major crack, after four-point bending tests. Microscopic images were taken from the cross sections of these cut specimens by using an optical microscope. Then these microscopic images were analyzed by using a tensor description method and fiber orientations in each of the x, y and z directions were obtained.

Results showed the importance of the formwork dimensions, hence effect of mould dimensions on the flow behavior, fiber orientation and resulting mechanical performance of the fiber-reinforced cement-based materials.

# TABLE OF CONTENTS

# LIST OF FIGURES

# LIST OF TABLES

# 1. INTRODUCTION

For more than 30 years ordinary concrete materials have been reinforced with short randomly distributed fibers [1,2]. The use of fiber-reinforced self-consolidating concrete (FRSCC) continues to increase all around the world due to its many advantages compared to traditional concrete. The advantages of FRSCC are basically related to its fresh state properties, which can be adjusted according to the needs of specific applications.

It is well known that FRC's can be used for lots of semi-structural and structural applications. For example, FRC is often used for thin elements like slabs, floors or roof elements if the passing of the reinforcement bars is rather difficult, due to dimensions of structures. Therefore, fibers substitute the rebars completely and act as a load bearing element. If fibers are compared to ordinary reinforcement, their small diameter with a high surface area can be uniformly dispersed resulting in a randomly distributed arrangement and therefore crack bridging potential.

On the other hand, use of fiber-reinforced cement-based materials for structural and semi-structural applications is hindered due to the lack of well-established codes/standards which define design principles. Efforts are being made for developing new standards to satisfy the needs of academia and industry. These documents are constituted as a result of years of experience of researchers and most of the information and generalized rules are proved by experimental studies. Therefore, the study of steel fiber-reinforced concrete can be named as an area, where significant efforts need to be focused.

Recent studies based on extensive experimental investigations highlight the fact that the strength and the ductility of reinforced concrete beams are enhanced by using FRC instead of ordinary concrete.

Effects of fiber addition on the ductile behavior, bearing capacity and shear strength of concrete have been studied in detail. Oh, B.H. [3] examined the increased ductility of beams by the addition of steel fibers. Another study by Campione [4], showed that the addition of fibers increases the bearing capacity of the beams and ensures more ductile

behaviour, at the same time reducing degradation effects under cyclic reversal loads. Results of the study of Lim et al. [5] showed that the first crack shear strength increases significantly as fibre content increases and the ultimate shear strength is also improved. Also, the results showed that steel fibres can greatly enhance the tensile properties of concrete and improve resistance to cracking. Increased ductility and flexural behavior of FRC beams were also studied by Chunxiang et al. [6]. The results showed that, the descending part of the load-displacement curve of the concrete beams without steel fibers is much steeper than that with steel fibers, which shows that the addition of steel fibers makes the high strength concrete beams more ductile.

The encouraging results of all those studies about FRC beams showed advantages of steel fiber-reinforced concrete, hence their results support the usage of steel-fiber reinforcement in structural applications.

There are many variables and parameters that should be taken into account since each of the resulting component/structure has different structural and geometrical properties and the “fiber-reinforced cement-based material” used to built so called component/structure is also different for each application. Several experimental and theoretical studies highlight the fact that the principal parameters influencing the structural response of reinforced concrete beams are: type (monotonic or cyclic) and direction (vertical or horizontal) of external loads; shear span to depth ratio; strength of concrete; shape and dimensions of members; type, grade and arrangements of longitudinal and transverse steel reinforcements. Depending on the combination of the mentioned above parameters, the ultimate loads and failure mode can change.

Features of different fibers used result in varying material properties, structural behavior and failure modes. Parameters such as fiber type, fiber geometry, fiber dimensions and fiber dispersion features enormously affect the material performance, as mentioned before. If structural design of fiber-reinforced materials is to be made, than the effect of fibers should be included into equations and predictions. For this, a well-established background is needed.

Research on fiber-reinforcement of cement-based materials has been done for the last 40 years and a remarkable literature on the subject can be found. However, more research is needed to quantify the effects of different fiber applications on the material performance. Further research is required for a comprehensive understanding and a more widespread use of fiber-reinforced cement-based materials.

Considering these factors, a comprehensive study is conducted in this thesis to better understand the material properties of FRCs in the fresh and hardened states. The challenges in this thesis are:

- To study the effects of mould constrictions on the alignment and dispersion features of fibers
- To find a relationship between the fresh and hardened state properties by defined parameters

Previous studies had shown the effect of flow direction on the alignment and distribution of fibers. Short cut discontinuous fibers had a tendency to align in the direction of flow and walls of formwork were found to act as barriers for the movement of fiber-reinforced materials. This effect is known but not examined.

The results obtained from previous studies highlight the need for further investigation of the strong connection existing between fibre dispersion, fresh state and mechanical properties of fibre reinforced concrete. However, there is not any study related with the effects of formwork dimensions on the fiber dispersion.

Therefore, the main objective of this study is to investigate the effects of formwork dimensions/constrictions on the flow and consequently alignment of fibers. Two parameters which are “formwork width/fiber length” and “formwork thickness/fiber length” were used for this purpose.

# 2. LITERATURE REVIEW

In this part a brief summary of the literature related with this research is given. First of all a more general literature of Fiber Reinforced Cement Based Materials is given. Following this, literature related with SFRC mix design, fiber dispersion analysis and mechanical performance of SFRC's are given.

## 2.1. Steel Fiber Reinforced Concrete

Concrete is a brittle material with low strain capacity and tensile strength. Usually fibers are incorporated into concrete to overcome this weakness by producing Fiber Reinforced Concrete (FRC) with increased tensile strength, ductility and toughness.

Fiber reinforced concrete may be defined as a composite material made with Portland cement, aggregate, and incorporating discrete discontinuous fibers. In the recent decades, steel fiber reinforced concrete (SFRC) became a very popular and attractive material in structural engineering because of its good mechanical performance. The most important advantages are preventing macrocracks, delaying microcracks propagation to macroscopic level and the improved ductility after formation of microcracks.

The general tensile behavior of concrete is demonstrated in Figure 2.1 [7]. Without any fiber reinforcement, the plain concrete matrix exhibits a strain-softening response with low tensile strength and ductility. Because, due to low fracture toughness of concrete, tensile cracks may easily occur when there is an applied stress. The interfacial bond developed between the fibers and matrix makes use of the strength and stiffness of the fibers in reinforcing the brittle matrix. Once the matrix cracks, load can be still transfered across the crack faces through the steel fibers. As the load on the composite is increased, the process of fiber pullout affects load carrying capacity and further contributes to energy dissipation. It has also been known that when using a high volume fraction of fibers with a high specific surface area, the crack bridging potential and the strength of the composite are increased [8],[9].

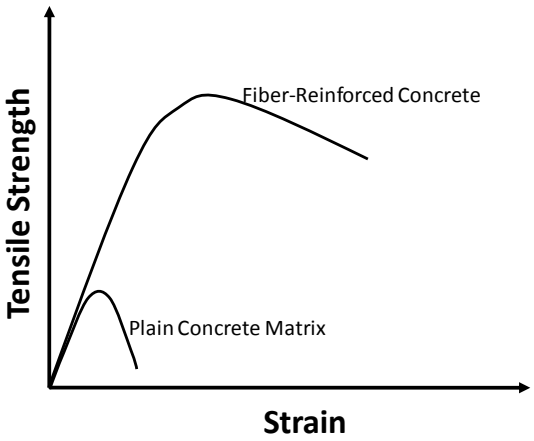


Figure 2.1. General tensile behavior of concrete

The role of randomly distributed discontinuous fibers is to bridge across the cracks that develop and this provides some post- cracking "ductility". If the fibers are sufficiently strong and well bonded to material. they permit the FRC to carry significant stresses over a relatively large strain capacity in the post-cracking stage.

In addition to that, use of fibers in concrete has led to numerous advantages in construction technology. It has been reported that fibers are effective in many ways, such as:

- Fiber reinforcement has been shown to improve flexural strength and shear strength of cementitious materials [10,11].
- Fibers bridge cracks during loading and transfer the load, arresting the growth and coalescence of cracks, playing the role of energy absorber [12,13].
- The fibers reduce the shrinkage, cracking and permeability of concrete [14].
- The fibers enhance fatigue and impact resistance [11,15].
- The fibers take up internal stresses through their tension resistance and hence ensure the transfer of the loads, provided that a good bond exists between the fibers and the hardened cement matrix [16,17].

A huge amount of both theoretical and experimental research has been done over the last years, based on the possibility of replacing conventional reinforcement with Steel Fiber Reinforced Concrete (SFRC) elements in structural applications. Among many well known advantages of steel fiber reinforcement, which may come from such a replacement,

what recognised was the possibility of having, randomly oriented fiber reinforcing elements, randomly spaced in the structure.
When the fiber reinforcement is in the form of short discrete fibers, they act effectively as rigid inclusions in the concrete matrix. Physically, they have thus the same order of magnitude as aggregate inclusions; steel fiber reinforcement cannot therefore be regarded as a direct replacement of longitudinal reinforcement in reinforced and prestressed structural members. [18]

On the other hand a large amount of both experimental and theoretical studies have been done over the last decades, dating back to 1972 [19], focusing on the possibility of replacing conventional reinforcement of with steel fibres in reinforced concrete elements.
Ferrara et al. [20] stated that among the several well known advantages which may come from such a replacement, what was quite early recognised was the possibility of having randomly oriented wirelike reinforcing elements, homogeneously spaced closer than the minimum distance obtainable with the smallest stirrups.

In these last few years, studies focusing on this replacement have shown that the achievement within a structural element of a homogeneous distribution of randomly oriented fibres, is a crucial point in respect of guaranteeing the structural performance with a suitable degree of repeatability. Governing the dispersion and the orientation of fibers in concrete through a suitably balanced set of fresh state properties and a carefully designed casting procedure, if proved effective, would hence be a feasible way to achieve a mechanical performance of the FRC which is optimal to the foreseen structural applications.[21] Therefore it is of the main importance that, the correlation between fibre distribution, fresh and hardened-state properties of SFRCs need further investigation, in regard to designing enhanced cement composites “tailored” for specific structural applications. [20]

## 2.2. SFRC Mix Design

As with any other type of concrete, the mix proportions for SFRC depend upon the requirements in terms of strength, workability, and so on. It's very important to have a well proportioned concrete, so that mixture behaves homogenously to keep fluidity, segregation resistance, durability and also acceptable mechanical properties.Several procedures for proportioning SFRC mixes are available, which mainly focuses on the workability of the resulting mix. However, there are some considerations that are particular to SFRC.

Choice of SCC when using fibers may be advantageous, since a better dispersion could be possible due to superior performance of SCC in the fresh state. [22] Therefore a more uniform dispersion of fibers can be obtained, which is very critical for a wider structural use of fiber-reinforced concrete.

An optimization procedure of the mix design for high performance FRC, to be employed for manufacturing roof elements where fibers as to serve as the only reinforcement has been assessed in the previous study of Ferrara et al [23] The procedure in that study was based on an investigation on the fresh state performance performed with mini-cone and Marsh cone tests. As a result of this study, they have stated that for optimizing a mix composition, the ability of the fresh concrete to well disperse and effectively drive steel fibers along the casting flow direction should be carefully evaluated.

Following this, Ozyurt et al. [24], studied the mix design for thin section fiber-reinforced cementitious materials. In that study, various self-consolidating fiber-reinforced mixes were tested for obtaining an acceptable static and dynamic segregation resistance, flowability characteristics and high overall performance.

## 2.3. Fiber Dispersion Analysis

Concrete is a weak material in tension, therefore considering a beam under loading, cracks in the specimen start from the micro-level with fine discontinuous microcracks distributed throughout the specimen. These cracks then become larger cracks with increasing stress and finally the specimen fails when the ultimate tensile stress is reached. Fibers control the starting of these microcracks and increase in their size and also control the cracks from the micro to the macro scale, depending on the size of fibers, by bridging cracks and delaying the sudden formation of larger cracks by coalescence [25].

With the increasing understanding of fiber reinforcement, the use of fibers has extended to partially load-carrying applications such as pavements, industrial floors, wall panels, and precast roof elements. [26, 27] Presently, in many structural applications, replacing conventional reinforcement with fibers is under consideration. There are some concerns and issues, however, that prevent the use of fibers in structural elements. One of the most important issues is the control of fiber dispersion.

To obtain good mechanical performance, the most important criteria is the control and characterization of fiber dispersion characteristics, since composite performance can be directly related to the effectiveness of fibers to control cracks.

Fiber addition to concrete for preventing cracks may have a positive effect on the mechanical properties, but since fibres may not all necessarily aligned in the direction of stress, the effectivity is debatable. It would be better to align fibres in the direction of stress, which leads to improved performance of FRC in a structure.

Effectiveness of fiber reinforcement is highly dependent on fiber dispersion and orientation. [28] Poor dispersion can cause poor fresh and hardened state properties, affecting the resulting overall performance of the structure. Therefore, fiber dispersion is an important factor that affects both fresh and hardened state properties of cement-based materials. Akkaya et al. [29] found that, if the fibers were well dispersed, material performance was improved. Therefore, investigating fiber dispersion is very important for

both fresh state and hardened state performance of FRC specimens. As a result, comprehensive research is needed so that fiber dispersion can be controlled and monitored.

Various methods have been used to monitor fiber dispersion. [30,31] Chermant et al. [32] illustrated the use of automatic image analysis techniques to measure some morphological characteristics of cement, concrete and fiber reinforced concrete (FRC). They used X-rays on iron ribbon fibers to establish their locations within the matrix. They suggested a covariance function of nearest-neighbor fibers to characterize their distribution.

Yang [33] stated that there are four methods for fiber dispersion analysis in FRC's. The fresh mixture method (FM method), the measurement of electrical resistance (ERM method), the scanning electron microscope method (SEM method) and the simulation experiment (SE method). He suggested that the simulation experiment (SE method) is the best method to determine the effect of various fiber dispersion agents. In addition to that, different methods can be fit for different conditions and they can also be used together to gain the true dispersion of fibers.

Akkaya [34] used SEM/optical microscopy method for locating short fibers and then applied statistical analysis to quantify fiber dispersion, with good results. Statistical methods from the theory of point processes were used in that study for describing fiber dispersion patterns by straightforward and easily calculated statistics.

In this study data from two-dimensional cross sections were used for orientation analyses and Image Analysis technique was used for analyzing fiber dispersion and a tensor description method was employed for fiber orientation density calculations in the specimens.

### 2.3.1. Image analysis

Image analysis is one of the most commonnly used and well-studied method for fiber dispersion analysis. Two dimensional or three-dimensional micrographs of specimens can be taken and studied using appropriate equipment and image analysis programs. This method is a trusted method when applied appropriately.

Chermant et al. [32], showed that automatic image analysis is a suitable tool to access to many morphological parameters. And, that should allow to stablish a beter understanding between morphological parameters and physical properties of civil engineering materials, such as fiber-reinforced concrete. Many illustrations of use of automatic image analysis were given in their paper [32] in order to quantify the morphology of the concrete matrix, microcracks and fibers in FRC. Therefore, it is suggested to be a suitable method for determining fiber dispersion and orientation in FRCs.

It was also shown in the study of Eberhardt et al. [35] that, fiber-orientation measurement by two-dimensional (2D) image analysis of polished cross-sections is a rapid and highly efficient method for determining the fiber orientation distribution over large sample areas.

As cocncluded from previous research, ,mage analysis is a basic method for examining micro-structural characteristics of materials. It can also be used for investigating fiber-dispersion analysis of FRCs. The method is based on obtaining microscopic images of sections to study dispersion of fibers. Either two dimensional or three dimensional microscopic images of specimens can be taken and analyzed using image analysis program.

The measurement of fiber dispersion by 2D image analysis requires the preparation of a cross-section. The method of preparation depends on the technique used to image the specimen, e.g. scanning electron microscopy (SEM). [35] As a result, the preparation of the concrete specimen for inspection by reflected light microscopy requires high contrast between the steel fibers and concrete matrix, which may not be achieved simply by polishing the specimen, but also grinding with emery paper for several layers.

The orientation of a fiber and the location of its intersection with the section plane are described by the parameters ($\theta$, $\varphi$) and ($x$, $y$), respectively. These parameters are straightforward to derive from an elliptical fiber cross-section by image analysis. The parameters that describe an ellipse are its position ($x_c$, $y_c$), axis lengths ($a$, $b$) and orientation, $\varphi$, as illustrated in Figure 2.2.

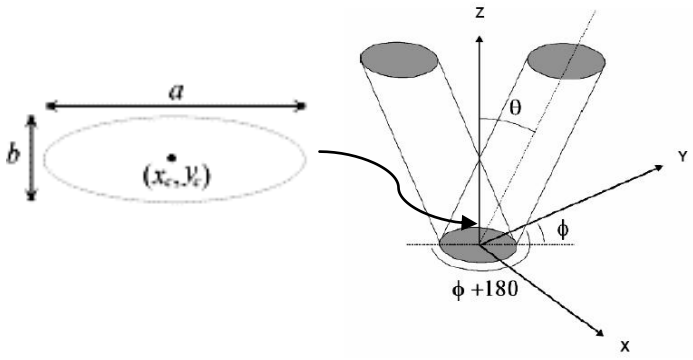


Figure 2.2. The position and orientation of a fiber can be determined from the parameters of its elliptical cross section (a, b, $x_c$, $y_c$, φ).

The calculations of orientation tensors are straightforward, and they give concise information about the fiber orientation density. Orientation tensors are obtained from moments of the orientation distribution function. The orientation of a fiber is derived from the parameters of its elliptical cross-section as follows:

$$\theta=\arccos \quad (1)$$

$$\varphi=\varphi \text{ or } \varphi+180 \quad (2)$$

The two possible values for φ are the result of an ambiguity in determining the orientation of a fiber, due to fibers with orientations φ and φ+180 having identical cross-sections. The diagonal components of the orientation tensor are unaffected by this ambiguity. [35]

In this study, by referencing the method of Eberhardt et al. [35], data from two dimensional cross-sections were used for fiber dispersion and orientation analyses and second order orientation tensors were used to calculate fiber orientation.

A tensor description method was employed for fiber orientation density calculations in the specimen. This method is widely used to describe fiber orientation distribution in fiber-reinforced composite materials such as short fiberreinforced polymers. A detailed description of the method is given in Part 4.1, Experimental Methods, Fiber Dispersion Analysis.

### 2.3.2. Segregation Analysis

Steel fibers have more density, compared with the cement paste or fresh concrete, therefore sometimes inhomogenous dispersion of fibers may occur in FRCs, due to improper mixing or gravitational settling. This improper alignment of fibers is called segregation and segregation can have a negative effect on structure performance where a constant tensile stress over the whole cross-section is expected. Nevertheless, whenever the homogeneous distribution and random orientation of fibers can be guaranteed within a fresh concrete, the casting into formworks and the compaction by vibration may also lead fibers to be oriented along preferential directions [36], with not a negligible tendency to segregation.

Previous study of Ozyurt et al. [37] showed that the segregation of the fibers increased with increasing vibration. And, SCC was found to be superior to conventional concrete, with the features such as high segregation resistance, good placeability, and high mechanical performance.Therefore, choosing Self-Compacting concrete for FRC mixes should be better for segregation resistance, since SCC doesn’t need any vibrations.

Fresh SCC must be stable to ensure the homogeneity of the mechanical strength of the structure. However, several problems like bleeding, settlement or segregation can ocur. Segregation is strongly related to composition of fresh concrete. The fresh concrete is usually considered as a non-Newtonian fluid since it is a mixture of aggregate, cement and water. The flow behavior of the fresh concrete to viscosity plays a crucial role in the quality of the high performance concretes. Fibers in fresh concrete usually cause segregation in the final product depending on the flow condition.

In the case of SCC, segregation may occur during transport, flowing into the moulds or after placement when the concrete is in a plastic state. This results in non-uniform distribution of fibers in self-compacting, steel fiber-reinforced concrete (SC-SFRC)

If segregation appears during placing of concrete, this refers to dynamic segregation and if it happens afterwards, during the dormant stage this refers to static segregation)[38].

2.3.2.1. Static Segregation: Segregation resistance is a critical functional requirement for self-consolidating concrete (SCC) during the fresh state. Because of its highly fluid nature, SCC is more susceptible to static segregation, compared to conventional concrete. Segregation is the tendency for fibers to separate from the sand-cement mortar, and static refers to segregation when the concrete is at rest. Static segregation consists of the sedimentation of the fibers of the fresh FRC under gravity forces, as seen in Figure 2.3 (a). Static segregation may occur after the SCC has been cast until it has hardened.

2.3.2.2. Dynamic Segregation: Dynamic stability refers to the resistance of concrete to separation during movement (e.g. mixing, placement into the formwork), as it is seen in Figure 2.3 (b). Adequate resistance of concrete to separation of constituents upon placement and spread into the formwork is required for SCC, when flowing through closely obstacles or constraints.

Once the concrete has been placed in the moulds and it is in a static state, the forces acting on the fibers can be calculated easily from Stokes' Law. However, during placing, and during horizontal flow, an aggregate particle is subjected to additional forces; the mixture drag and vertical drag that help to keep the particle suspended and flowing in the mixture. The mixture drag is proportional to the square of velocity of the mixture and the square of the particle diameter, whereas, the vertical drag is proportioned to the velocity of the mixture and the fiber dimensions. Consequently, as the velocity of the mixture is increased, the resistance to dynamic segregation is also increased.

In the last years, it was acknowledged that an SFRC material with high performance should have high static and dynamic segregation resistance. Because, as a result of segregation, there will be an inhomogenity in the distribution of fibers, which may lead to some fiber free areas will occur in the specimens.

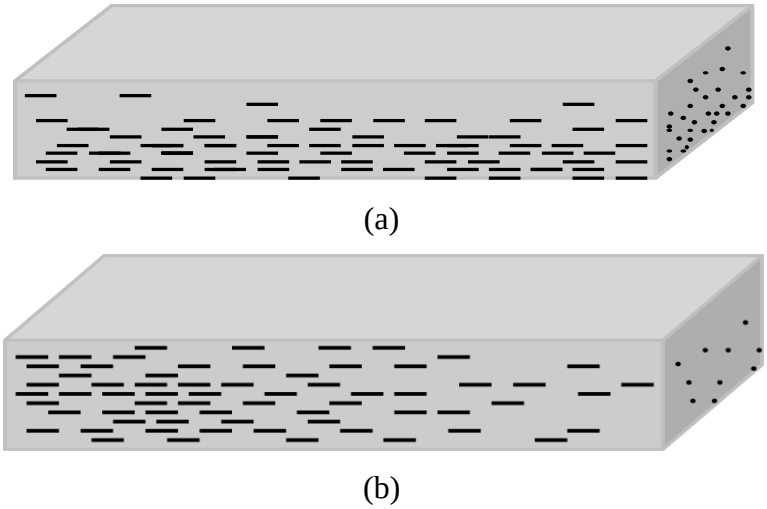

(a)

(b)

Figure 2.3. (a) A representation of static segregation of fibers in a FRC beam, (b) A representation of dynamic segregation of fibers in a FRC beam

Previous work of Akkaya et al. [29] demonstrated that the fiber free areas in FRCs can act as flaws; crack initiation and propagation is favored in the fiber-free areas, leading to reduced strength and toughness.

A crack initiates and advances from the section of a composite that has larger fiber-free matrix areas. [29] Therefore, size and amount of this fiber free areas have an important role in the initiation and propogation of the cracks in the specimen. As a result, segregation is an important problem for FRC's and need to be examined in detail, in order to have satisfiying mechanical performance.

## 2.4. Mechanical Performance of FRC's

Behavior of fresh concrete can eventually have significant effects on mechanical performance of hardened concrete. Therefore, examining fresh state behavior of concrete and fiber orientation has importance on determining mechanical performance of FRCs.

Steel fibers are generally found to have much greater effect on the flexural strength of SFRC than on either the compressive or tensile strength, with increases of more than 100% having been reported. The increase in flexural strength is particularly sensitive, not only to the fiber volume, but also to the aspect ratio of the fibers, with higher aspect ratio leading to larger strength increases.

Fibers are added to concrete not only to improve the strength, but primarily to improve the toughness, or energy absorption capacity. Commonly, the flexural toughness is defined as the area under the complete load-deflection curve in flexure; this is sometimes referred to as the total energy to fracture. Alternatively, the toughness may be defined as the area under the load-deflection curve out to some particular deflection, or out to the point at which the load has fallen back to some fixed percentage of the peak load.

Fresh and hardened state properties of FRC specimens were connected by means of fiber dispersion and orientation. In the previous studies, fresh state properties were found to affect segregation and dispersion of fibers and therefore mechanical performance of FRC. [39]

It was observed that preferred orientation of fibers results in non-homogenous material properties throughout a specimen. Therefore, it was concluded that the mechanical performance of composite materials may vary in different parts of the specimen. Consequently both fiber dispersion analysis and four-point bending tests should be performed for clearly understanding the effects of fiber orientation on mechanical performance.

The results obtained from all these studies highlight the need for further investigation of the strong connection existing between fiber distribution and therefore

mechanical properties of fiber reinforced concrete. [20] Carrying out a detailed study on various formwork and fiber dimensions, in terms of both fresh state and hardened state performance would be a remarkable improvement for figuring out this connection between fiber distribution and mechanical properties of FRC's.

### 2.4.1. Four-Point Bending Test

Four-point bending tests were performed to study the effects of fiber orientation on mechanical performance. Tests were carried out on unnotched specimens in order to classify and characterize the SFRC tested. Four-point bending tests are usually performed to investigate fibers performances and to evaluate their possible use for the design of structural members, by means of the derivation of ductility and tenacity of the material according to standards [40].

The addition of steel fibers significantly improves many of the engineering properties of mortar and concrete, notably impact strength and toughness [41]. The improved fresh state and mechanical performance of fiber-reinforced concrete comes from its increased capacity to absorb energy during fracture. An unreinforced concrete shows a brittle behavior, at the occurrence of cracking stresses during failure. On the other hand, the ductile fibers in fiber-reinforced concrete continue to carry stresses even after the cracking of matrix, which helps providing structural integrity and unity.

Further, if properly designed, fibers undergo a pullout process, and the frictional work needed for pullout leads to a significantly improved energy absorption capability. This energy absorption attribute of SFRC is often termed "Toughness". [42] The importance of fiber geometry and matrix strength on the toughness characteristics of SFRC has been clearly established by earlier researchers [43, 44].

Performance of fiber-reinforced concrete is affected in different ways by the amount and aspect ratio of fibers in the concrete. As mentioned in ASTM C1609, in some cases, fibers may increase the residual load and toughness capacity at specified deflections while producing a first-peak strength equal to or slightly greater than the flexural strength of the concrete without fibers. In other cases, fibers may significantly increase the first-

peak and peak strengths while affecting a relatively small increase in residual load capacity and specimen toughness at specified deflections. [45]

The first-peak strength characterizes the flexural behavior of the fiber-reinforced concrete up to the onset of cracking, while residual strengths at specified deflections characterize the residual capacity after cracking. [45]

Boulekbache et al. [46] mentioned that a cracked concrete can continue to support further increases in loading without widening the crack width through fiber crack stitching and through the deformation of the fibres, which causes increased crushing and splitting of the matrix. And as a result, at the end of the loading stage, failure is very ductile and soft since most of the energy is absorbed by the deformed fibres. For the fiber reinforced concrete, more than one peak load may occur, one at the end of the cement matrix contribution and others when the fibres reach their ultimate capacity.

Specimen toughness is an important parameter for determining mechanical performance of the specimens, since it measures the energy absorption capacity. The results of this test method are used for comparing the performance of various fiber-reinforced concrete mixtures or in research and development work. [45] They may also be used to monitor concrete quality, to verify compliance with construction specifications, obtain flexural strength data on fiber-reinforced concrete members subject to pure bending, or to evaluate the quality of concrete in service.

### 2.4.2. Flexural Toughness

Steel fiber reinforced concrete (SFRC) is distinguished from plain concrete by its ability to absorb large amount of energy and to undergo large deformations before failure. The preceeding characteristics are referred to as toughness. Flexural toughness can be measured by taking the area under theload-deflection curve in flexure.

The addition of steel fibers to concretenot only results in a large increase in flexural strength, but also a considerable increase in toughness. After cracking, the cracks can not extend without stretching and debonding of the fibers. As a result, a large additional energy

is absorbed before complete separationof the specimen occurs. Toughness can be measured in various ways.

There are, however, a number of uncertainties regarding how FRC flexural toughness should be measured, interpreted, or used. Various flexural toughness test methods have been developed in different countries. ASTM-C1018, JSCE-SF4, and NBP No. 7 are three of the most commonly used test methods.

Lianrong et al. [47] studied the effects of testing and material variables on both the load-deflection response and the flexural toughness of FRC, investigated the reproducibility of the flexural toughness test methods of FRC discussed difficulties in toughness evaluation, defined various flexural toughness parameters, assessed relative advantages and disadvantages of different methods of characterizing toughness, and developed recommendations for a more suitable procedure for FRC flexural toughness evaluation. Finally, he stated that the load-deflection response of FRC is an experimental property and so are the flexural toughness parameters derived from the response, and depend not only on material variables but also on testing factors.

Out of various testing variables, the deflection measuring system, the loading system, and specimen size/geometry are the three most important factors; while amongst the various material variables, fibre content and fibre type/profile are the most important. The major difficulties in measuring the load-deflection response, caused by either extraneous deformations, first crack determination, or instability, has much more significant effects on ASTM toughness parameters than on JSCE toughness parameters. [47] As stated by Lianrong [47], ASTM parameters may not be particularly sensitive in distinguishing either amongst different fibre contents for SFRC with similar low fibre contents, whereas JSCE parameters are more sensitive in this regard.

An accurate measurement of deflection is very important to characterize toughness of FRC.[42] Calculation of toughness indexes requires an accurate assessment of the first-crack energy, which constitutes the denominator in the definition of the various indexes. In addition, it is mentioned by Nataraja et al. [42] that the identification of first-crack

deflection is not so simple with ASTM method, due to the substantial non-linearity of load deflection curves even prior to attaining the peak load.

Identifying the correct occurrence location of the first crack, which is crucial and one of the main problems with the ASTM method, is not a concern with the JSCE method. Unlike the ASTM method, the instability in the load-deflection plot right after the first crack is not of major concern in the JSCE method, since the end point deflection of span/150 is too far out in the curve to be affected by the instability in the initial portion.[42]

However, as mentioned by Nataraja et al., JSCE technique is sometimes criticized for the chosen deflection of span/150, as it is considered excessive for many applications. Since this deflection is purely arbitrary, any other suitable limit can be used based on the serviceability requirements, and the method can still be used.

And the main advantages of JSCE are that it is a simple method and flexural toughness can be determined easily by using any deflection measuring technique, without using any sophisticated instrumentation for determining the toughness factor. And in this method, determination of first crack, which is very difficult to identify, is not required. Furthermore, it was suggested by Nataraja et al. that the flexural toughness factor calculated using this approach has good correlation with the fiber-reinforcing index, which is ($V_f$.L/$d_f$), where $V_f$ is volume fraction of fibers, L is fiber length and $d_f$ is fiber diameter.

Therefore, considering the reliability and efficiency of various toughness parameters, JSCE SF-4 method was used for toughness calculations in this study.

# 3. EXPERIMENTAL STUDIES

## 3.1. Materials and Mix Design

Concrete mix used is adapted from one of the previous studies of Ozyurt et al. [24]. In previous study of Ozyurt et. Al [24] the mix design for a fiber-reinforced cement-based material was optimized for thin section precast elements. Different self-consolidating fiber-reinforced mixes were experimentally examined and mixes which showed the best performance was chosen in that study. In this study, mix designs were calculated based on the previous study's results.

### 3.1.1. Materials

3.1.1.1. Cement: The cement used for concrete specimens was CEM I 42.5 R, which was produced by Akcansa. Physical, mechanical and chemical properties of this cement is as following.

Table 3.1. Physical properties of cement

| **Physical Properties** | | |
|---|---|---|
| Specific Gravity | (g/cm³) | 3,14 |
| Initial Setting Time | (min.) | 139 |
| Final Setting Time | (min.) | 194 |
| Le Chatelier | (mm) | 0 |
| Specific Surface | (cm²/g) | 3870 |
| Residue on 45µm sieve | (%) | 5,9 |
| Residue on 90µm sieve | (%) | 0,4 |

Table 3.2. Mechanical properties of cement

| **Mechanical Properties** | | |
|---|---|---|
| ***Mechanical Properties/ day*** | ***Standards*** | ***Test Results*** |
| Early Strength 2 day | ≥ 20 Mpa | 30,5 |
| Early Strength 7 day | - | 46,0 |
| Standard Strength 28 day | ≥ 42,5 Mpa | 59,3 |
| | ≤ 62,5 Mpa | |

Table 3.3. Chemical properties of cement

| Chemical Properties | | |
|---|---|---|
| $SiO_2$ | (%) | 19,67 |
| Insoluble Residue | (%) | 0,3 |
| $Al_2O_3$ | (%) | 4,45 |
| $Fe_2O_3$ | (%) | 3,43 |
| CaO | (%) | 64,31 |
| MgO | (%) | 1,12 |
| $SO_3$ | (%) | 2,99 |
| Loss on Ignition | (%) | 2,24 |
| Cl | (%) | 0,0412 |
| $Na_2O$ /$K_2O$ | (%) | 0,21 - 0,76 |
| Tayin edilemeyen | (%) | 0,78 |
| S.CaO-Free Lime | (%) | 1,15 |
| Mineralogical Composition | $C_3S$ | 64,24 |
| | $C_2S$ | 8,02 |
| | $C_3A$ | 6 |
| | $C_4AF$ | 10,44 |
| LSF | | 0,99 |

3.1.1.2. Slag: The slag used for concrete specimens was produced by Akcansa. Chemical and physical properties of this slag is as following.

Table 3.4. Chemical properties of slag

| Chemical Properties | |
|---|---|
| $Ca\ CO_3 + Mg\ CO_3$ | - |
| $H_2O$ | 0,1 |
| Insoluble | - |
| $SiO_2$ | 45,12 |
| $Al_2O_3$ | 10,63 |
| $Fe_2O_3$ | 1,12 |
| CaO | 35,12 |
| MgO | 6,24 |
| S | 0,3 |
| $Na_2O$ | 0,2 |
| $K_2O$ | 1,23 |
| Cl | 0,0185 |
| Loss on Ignition | 0 |
| | |
| Total | 99,98 |

Table 3.5. Physical requirements of slag

| Physical Requirements | | |
|---|---|---|
| Specific Gravity | (g/cm³) | 2,92 |
| Specific Surface | (cm²/g) | 4240 |
| Residue on 45µm sieve | (%) | 1 |
| Residue on 90µm sieve | (%) | 0 |
| Residue on 200µm sieve | (%) | 0 |
| Activity Test Value | (N/mm²) | 12,4 |

3.1.1.3. Sand: Specific gravity of the sand used for concrete mixtures was 2,65 g/cm³ and grain diameter size less than or equal to 1mm.

3.1.1.4. Steel Fibers: Specific gravity of steel fibers used for concrete mixtures was 7,17 kg/m³. Two types of these steel fibers were used, one of them having 6mm length and the other one 13mm length. Both of these fibers have the same diameter of 0,16 mm.

3.1.1.5. Superplasticizer: A new generation of superplasticizer, called GLENIUM 51, having 1,075 kg/m³ specific gravity, was used 1,2-1,3 % in the concrete mixtures. This superplasticising admixture based on chains of modified polycarboxylate ether. It provides flowable concrete with the lowest water/cement ratio without segregation or bleeding. When compared to to traditional superplasticizers, the addition of GLENIUM 51 will improve the physical properties and thus the durability of concrete.

### 3.1.2. Mix Design

This mix was proved to have high overall performance. The mix proportions of the fiber-reinforced SCC used was as follows. Cement: Sand: Slag: Water: Plasticizer: Fiber: 524 :1229 :440 :235 :21 :100 kg/m$^3$. Two different length of a short cut steel fiber were used (6mm and 13mm). Both fibers had a diameter of 0,16mm. A polycarboxylate based hyperplasticizer is used for all mixes.

### 3.2. Formwork Dimensions

First of all, three different sizes of moulds have been prepared, in order to obtain various flow behaviors under different constraints. Moulds were designed to have same length (500 mm) and depth (50mm), but different widths of 100 mm, 200mm and 300mm as seen in Figure 3.1. Therefore the first parameter, which was pre-defined to be "flow width/fiber length" varied as is seen in Table 3.1. Two different mixes were cast by varying fiber length. Specimen thickness was also varied to be either 25mm or 50mm and the 2nd parameter which was determined to be "flow thickness/fiber length" varied from 1,9 to 8,3 as is seen in Table 1.

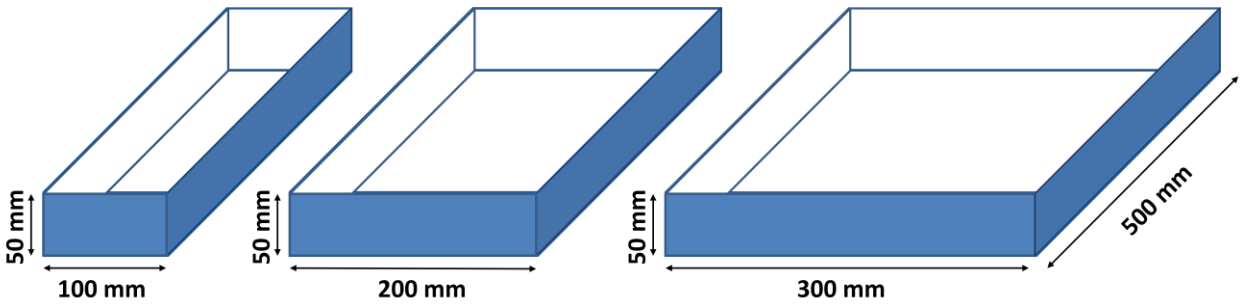


Figure 3.1. Formwork dimensions

Table 3.6. Parameters investigated in the scope of the study

| **Fiber length (mm) / Flow width (mm)** | **6** | **13** | |
|---|---|---|---|
| 100 | 16,7 | 7,7 | Formwork or flow width/fiber length (w/fL) |
| 200 | 33,3 | 15,4 | |
| 300 | 50 | 23,2 | |
| **Flow thickness (mm)** | | | |
| 25 | 4,2 | 1,9 | Formwork thickness/fiber length (t/fL) |
| 50 | 8,3 | 3,9 | |

As a result 4 groups of specimen were obtained, having 100mm, 200mm and 300mm widths. The specimens were numbered according to their thickness and fiber lengths. (i.e: For the 1st group, the specimens were named as 25/06, the number on the left hand side implying the specimen thickness and the number on the right hand side showing the fiber length). Specimens were demoulded the day after casting and cured for 28 days minimum.

Videos of flow were recorded during casting, in order to examine the variety in flow lines according to the mould sizes. A simple representation of the expected FRC flow lines was made and given in Figure 3.2. This figure is based on visual observations. Self compacting concrete mix was cast from one end of the moulds and left to flow to the other end until the mould is full. From the representation below it can be hypothesized that alignment of fibers in the flow direction may be higher in the single (S) specimens when compared to double (D) and triple (T) specimens due to formwork constrictions. Therefore specimens shown with (S) are expected to perform better under bending load.

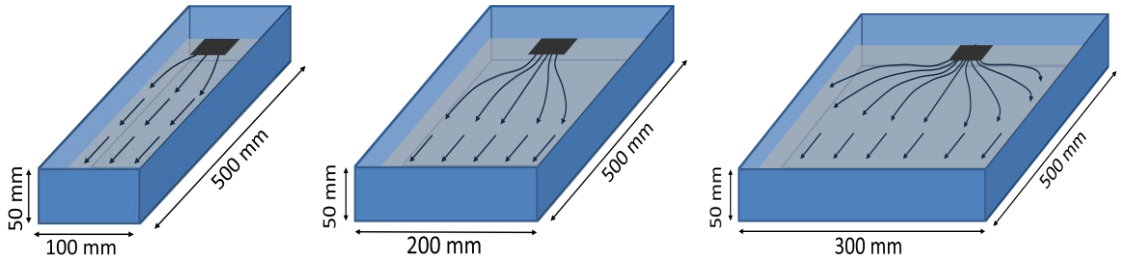


Figure 3.2. Predicted flow lines

Before exposing to any mechanical tests, the 200mm-width specimens were cut into two and the 300mm-width specimens were cut into three, in order to make all the specimens have the same width of 100mm (Figure 3.3).

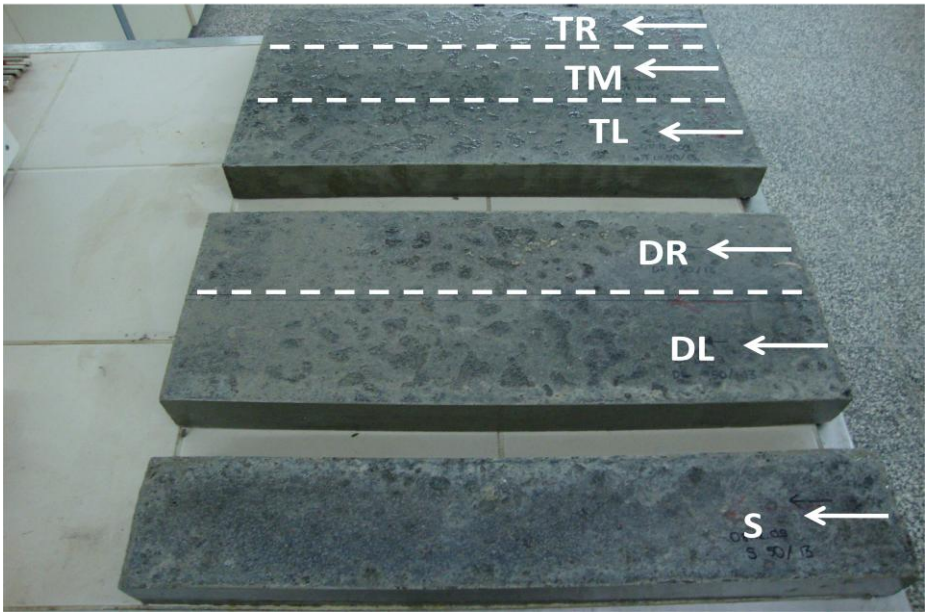


Figure 3.3. Beam specimens before cutting procedure

### 3.2. Determination of Specimen Codes

After that, each specimen was named accordingly (Figure 3.4). “S”, representing single for 100 mm-width specimens, “DR” and “DL” representing Double Right and Double Left parts for 200 mm-width specimens, and “TR”, “TM” and “TL” representing Triple Right, Triple Middle and Triple Left parts according to the flow direction for 300 mm-width specimens. Finally, total number of 24 specimens, (12 having 25x100x500 and 12 having 50x100x500 dimensions) were obtained.

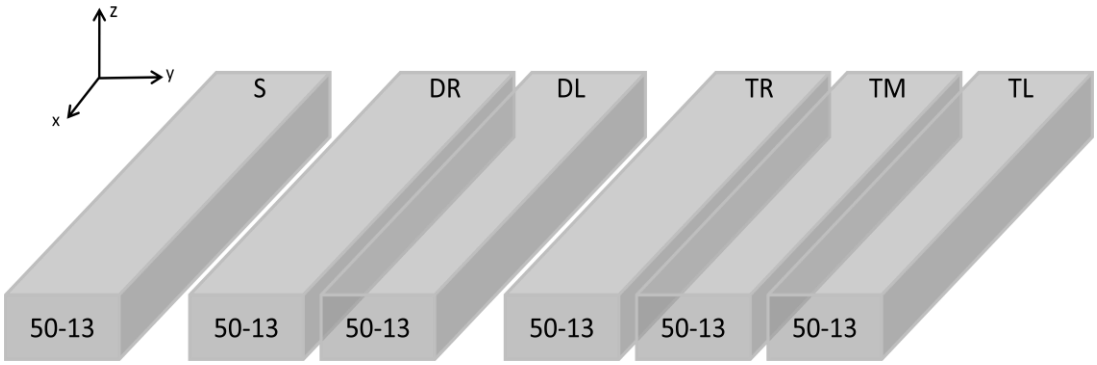


Figure 3.4. Representation of Group 50/13 of specimens and specimen codes

# 4. EXPERIMENTAL METHODS

## 4.1. Fiber Dispersion Analysis

Control and monitoring of fiber dispersion features are very important for obtaining desired results from the materials. Dispersion features of fibers dominate the properties of materials and affect the structural performance. Therefore quantification and modeling of fiber dispersion is very important for design purposes. In this study, the use of self-consolidating concrete (SCC), may be helpful in guaranteeing a uniform dispersion of fibers, because of its rheological stability and self-placability

Image analyses were used to evaluate fiber dispersion features of the specimens produced in this study. Image analysis is a well-understood and trusted method and proved to give reliable results. Important fiber dispersion features in this study were considered to be fiber segregation and fiber alignment/orientation. Sections next to the main cracks formed after four-point bending tests were chosen to obtain most representative results. A visual examination of the cross-sections was first made. No significant sign of fiber segregation was found.

The SCC mix used in this study was adopted from a previous study of the authors as mentioned before and it was specifically optimized to obtain high segregation resistance (Ozyurt et al., 2009). Segregation was not the main concern, but it was still checked in the cross-sections, which were examined to quantify the fiber alignment/orientation. To quantify the orientation of fibers a tensor description method, which is widely used in the fiber-reinforced polymer composite industry was used. Application of this method to the fiber-reinforced cement-based materials was done by Ozyurt et al. [37]. Details of the procedure applied could be found elsewhere (Advani and Tucker, 1987) [48]. A short introduction to the method will be given here.

The orientation state of a single fiber can be defined using in-plane ($\varphi$) and out of plane angles ($\theta$), as seen in Figure 4.1 and represented by Equation 1.

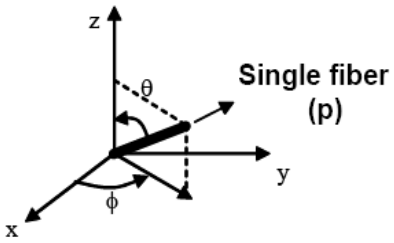


Figure 4.1. Orientation state of a single fiber

$$a_{ij} = \frac{\sum (p_i p_j)_n F_n}{\sum F_n} = \begin{pmatrix} a_{xx} & a_{xy} & a_{xz} \\ a_{yx} & a_{yy} & a_{yz} \\ a_{zx} & a_{zy} & a_{zz} \end{pmatrix} \quad \text{i,j = x, y, z} \tag{3}$$

In equation 1, $a_{ij}$ stands for the components of the orientation tensor; $p_x$, $p_y$, and $p_z$ and give the orientation state of a single fiber in reference directions and are calculated as follows.

$$p_x = Sin\theta Cos\phi, \quad p_y = Sin\theta Sin\phi, \quad p_z = Cos\theta \tag{4}$$

In-plane (φ) and out-of-plane (θ) angles for every fiber were measured using an image analysis program. $F_n$ in Eq. 1 gives the weighing function which is used to account for the effect of fiber orientation on the probability of a fiber being intercepted by the cross section under consideration. The probability of intercepting a fiber that is aligned vertical to the cutting plane is much higher compared to a fiber aligned parallel to the section. $F_n$ is calculated by using Equation 3.

$$F_n = \frac{1}{LCos\theta} \text{ for } \theta < \theta_c, \quad F_n = \frac{L}{d} \text{ for } \theta > \theta_c \text{ and } \theta_c = \arccos\left(\frac{d}{L}\right) \tag{5}$$

In this study, the orientation densities in the reference directions were needed. Therefore, only the main diagonal components of the tensor were calculated to obtain the alignments in the X, Y and Z directions, respectively.

## 4.2. Mechanical Performance

In order to assess the correlation between the mechanical performance of the fibre reinforced cementitious composite and the orientation of the fibres as due to the casting process, the beam specimens were tested in four-point bending, according to the test set-up shown in Figure 4.2 by using an MTS Closed-Loop Displacement Controlled Dynamic Testing Machine with 100 kN capacity. Loading was applied in displacement control, which was monitored using 4 LVDTs (Linear variable displacement transducer) that had a maximum range of ± 25 mm. Four displacement read-outs were monitored and average of the 4 values were used to draw load vs. deflection curves of the specimens.

For measuring crack opening displacement (COD), 2 LVDTs were placed horizontally on the sides of specimens and average of these 2 values were used to draw Load vs. COD curves, in order to gain more information about crack behavior, in addition to Load vs. deflection curves.

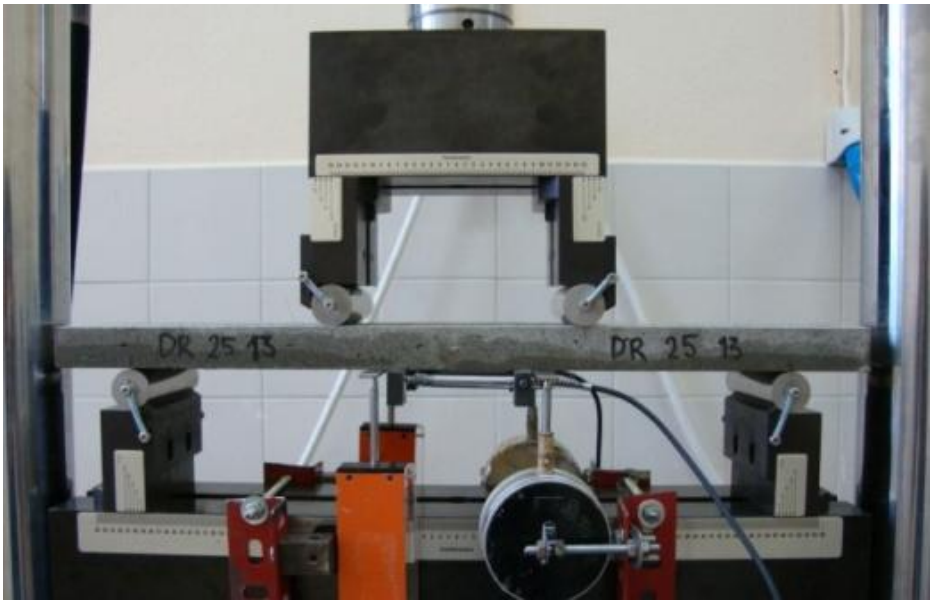


Figure 4.2. Four-point bending test setup

Loading setup is given in Figure 4.2. Span length (L) was 400 mm and gap between the loading heads was 150 mm. Geometry of a 25 mm thick specimen, support and loading position is shown representatively in Figure 4.3

.

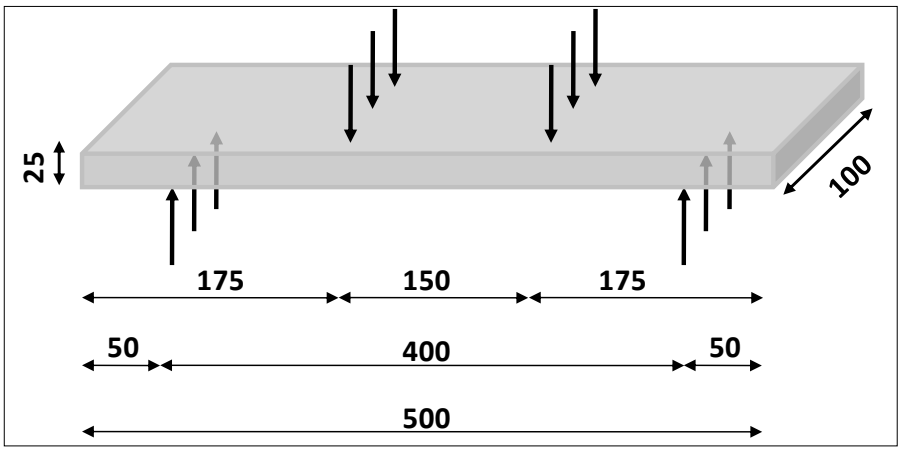


Figure 4.3. Geometry, support and load position

Loading was performed controlling the displacement of the machine actuator, which was applied at a rate of 0.1 mm/min. Testing continued until approximately 10 mm vertical displacement was reached.

Toughness of the specimens was evaluated according to JSCE standard SF-4 method. In this SF-4 method, the area under the load vs. deflection curve up to a deflection of a value equal to the L/150 is obtained. From flexural toughness results, a flexural toughness factor (FT) is calculated. This method is considered to be more representative and less susceptible to evaluation errors when compared to the toughness indices suggested in ASTM C 1018 (Nataraja et al., 2000). It was possible to obtain deflection values up until 10mm and therefore area under the curve with an end point deflection of 10mm was used when calculating Flexural Toughness (FT), instead of using L/150 value as the end point deflection. The JSCE SF-4 equation for flexural toughness is as following in Eqn.4:

$$FT = \frac{A_{(L/150)} \cdot L}{(L/150) b h^2} \tag{6}$$

where, A is the area under Load-Deflection curve (mm²), L is the span length (mm), b is the width of the specimens (mm) and h is the thickness of specimens (mm).

In this study, since end point deflection values for specimens were about 10 mm, $A_{(L/150)}$ value was taken as the area under the load vs. deflection curve upto 10 mm deflection.

# 5. RESULTS AND DISCUSSIONS

## 5.1. Fiber Dispersion

### 5.1.1. Effect of Mould Constrictions on the Fiber Dispersion State

To do fiber alignment analyses, beam specimens were cut into 2 pieces following four-point bending tests. Cutting was done near the major crack to obtain a representative information about the fiber dispersion state right next to the major crack, as seen in Figure 5.1.


Figure 5.1. Crack region, where specimens cut for image analysis

The preparation procedure includes the cutting of the specimen near the fracture zone. Although the specimen was cut so as to give a view of the fracture, the actual crack departed from one side of the cross section and did not pass close to the fibers on the opposite side of the cross section. Obtaining a smooth, clear surface of the specimens is important, since the appearance of their surfaces in the reflecting light microscope is determined by their reflection behaviour or, in other words, their roughness. Therefore, cross section surfaces rubbed by emery paper.

After that, microscopic images were taken from the cross sections by using an optical microscope. Then the fiber cross sections were marked on the image file in Adobe Photoshop, and the center coordinates of each fiber location were found using the ImageJ image analysis program. Then these microscopic images were analyzed by using a tensor

description method as summarized in 3.1. Considering the time, associated with the image processing, it was decided to choose some representative sections from single, double and triple samples of each group and the orientation density analyses were carried out on these subsections. The selected sections are from S, DL, TL, TM (making 12 sections in total), DR and TR sections were eliminated since nearly the same orientation results were expected from DR-DL and TR-TL sections due to the symmetry. Figure 5.2 shows examples of both thin and thick cross sections examined, position of the sections relative to X direction and sub-sections.

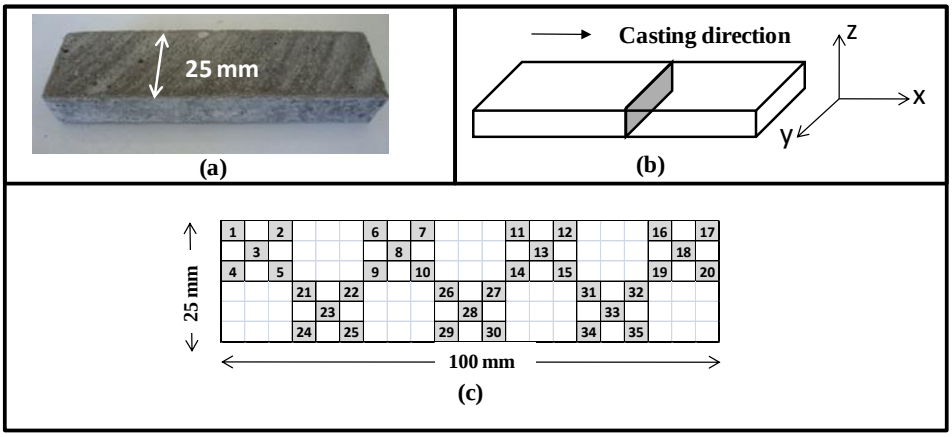


Figure 5.2. a) a sample 25 mm cross-section examined for the fiber alignment analysis, b) cutting direction of sections, c) sub-sections selected for analyses

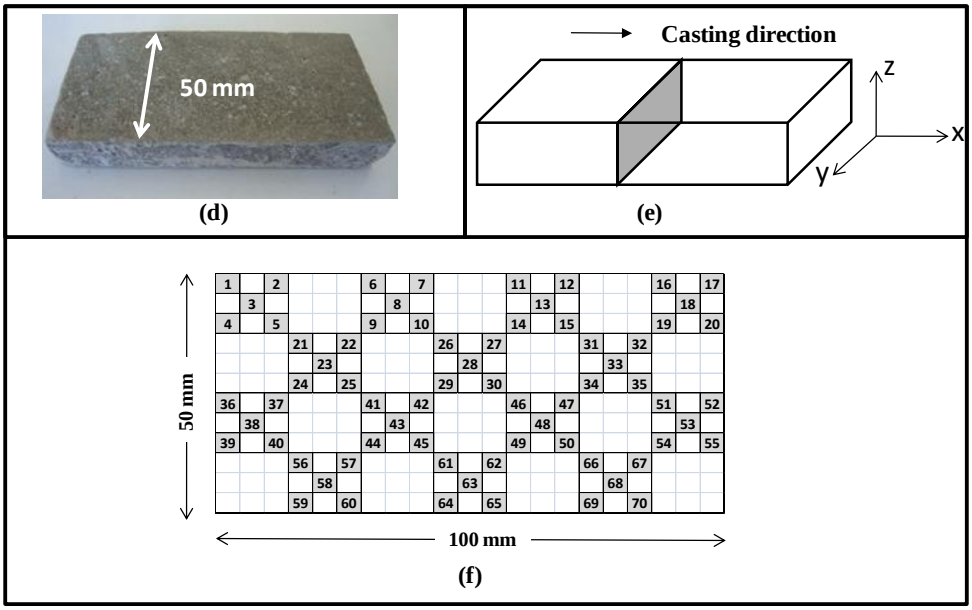


Figure 5.2. (contd.) d) a sample 50 mm cross-section examined for the fiber alignment analysis, e) cutting direction of sections, f) sub-sections selected for analyses

As a result of image analysis, fiber orientations in each of the x, y and z directions were obtained for S (single), DL (double left) and TL (triple left) specimens and given in Table 5.1.

Table 5.1. Fiber Orientation density results and variation of w/fL and t/fL parameters for the specimens

| Specimen | | | x | y | z | w/fL | t/fL |
|---|---|---|---|---|---|---|---|
| S | 25 | 6 | 0,703 | 0,165 | 0,132 | 16,7 | 4.2 |
| DL | 25 | 6 | 0,672 | 0,177 | 0,151 | 33,3 | |
| TL | 25 | 6 | 0,659 | 0,184 | 0,156 | 50,0 | |
| TM | 25 | 6 | 0,660 | 0,177 | 0,163 | 50,0 | |
| S | 50 | 6 | 0,707 | 0,148 | 0,144 | 16,7 | 8.3 |
| DL | 50 | 6 | 0,664 | 0,158 | 0,177 | 33,3 | |
| TL | 50 | 6 | 0,618 | 0,199 | 0,183 | 50,0 | |
| TM | 50 | 6 | 0,626 | 0,197 | 0,177 | 50,0 | |
| S | 25 | 13 | 0,568 | 0,235 | 0,197 | 7,7 | 1.9 |
| DL | 25 | 13 | 0,588 | 0,197 | 0,216 | 15,4 | |
| TL | 25 | 13 | 0,496 | 0,311 | 0,193 | 23,2 | |
| TM | 25 | 13 | 0,562 | 0,223 | 0,214 | 23,2 | |
| S | 50 | 13 | 0,632 | 0,151 | 0,217 | 7,7 | 3.9 |
| DL | 50 | 13 | 0,601 | 0,177 | 0,223 | 15,4 | |
| TL | 50 | 13 | 0,547 | 0,206 | 0,247 | 23,2 | |
| TM | 50 | 13 | 0,551 | 0,234 | 0,215 | 23,2 | |

### 5.1.2. Effect of Specimen Width on the Fiber Dispersion State

Variation in the fiber orientation densities (FOD) in the casting direction (x-dir.) of specimens having 6 mm fibers are shown in Figure 5.3 (a) and variation in the fiber orientation densities (FOD) in the casting direction (x-dir.) of specimens having 13 mm fibers are shown in Figure 5.3 (b) respectively.

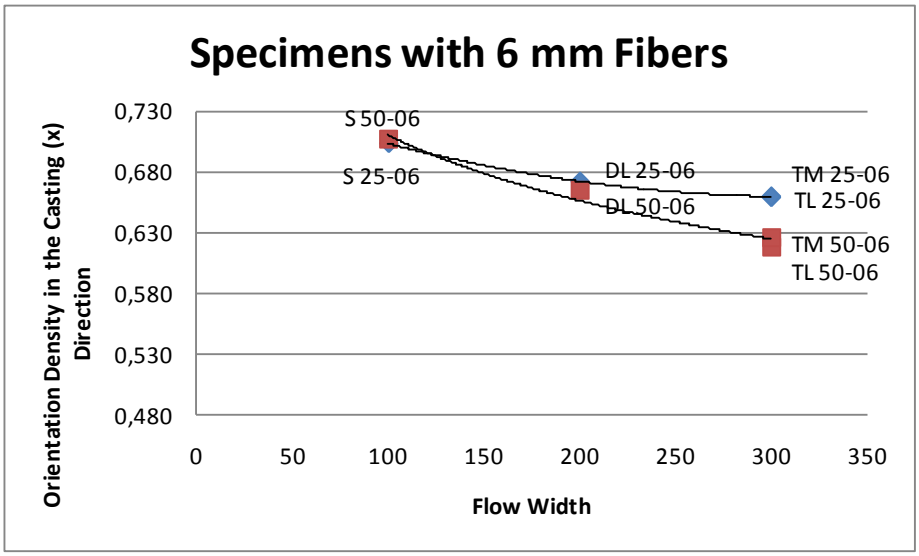


(a)

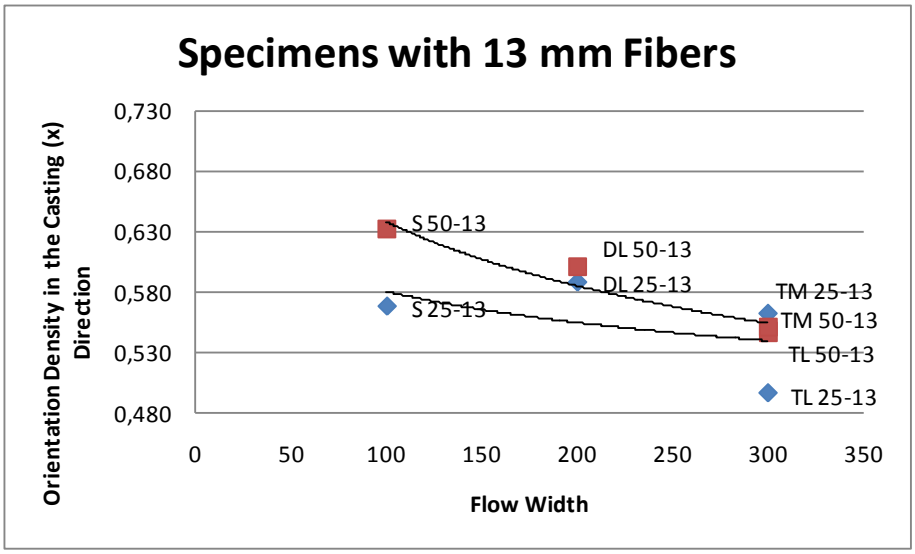


(b)

Figure 5.3. (a), (b) Effect of w/fL on the FOD of specimens having 6 mm and 13 mm fibers

This difference in the alignment of specimens having same mixture proportions, same fiber content and same thickness is only due to their initial formwork widths, in which casting has been done. Formwork widths of S, DR and DL specimens were less than TL, TM and TR specimens; therefore there were less space for fibers to flow freely in single (S) and double (D) specimen formworks compared with triple (T) specimens. This flow width constraint caused nearly 1D flow in single (S) and double (D) specimens, therefore fibers aligned in casting direction (x-dir) were more that of double (D) and triple

(T) specimens. Because, fibers have more free space to move with an increase in flow width.

Figure 5.4 shows variation in the orientation densities in the X direction with an increase in pre-defined w/fL parameter. As can be seen in Table 5.1 and Figure 5.4, fibers have the tendency to align in the flow direction and density of alignment decreases with an increase in specimen width (flow width/fiber length).

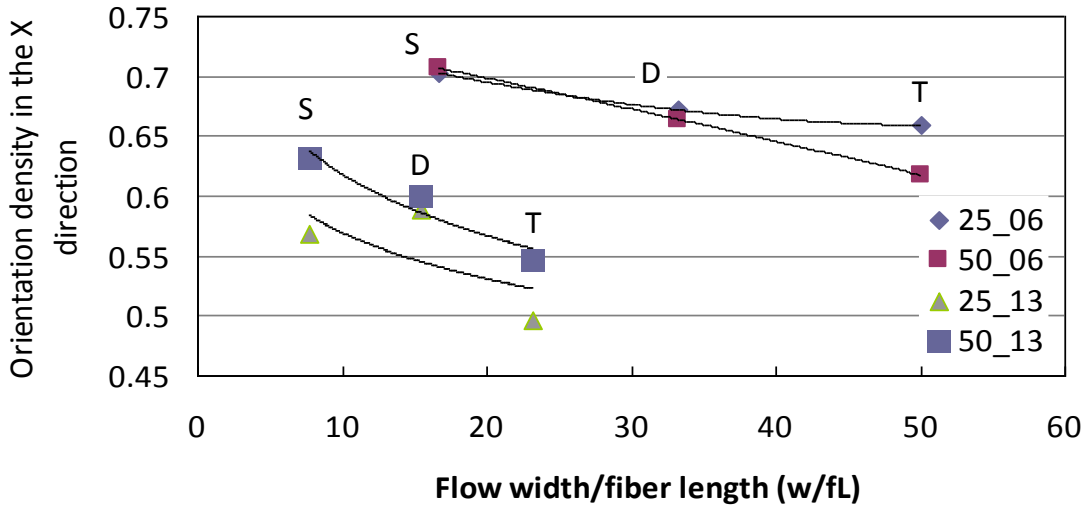


Figure 5.4. Effect of flow width/fiber length ratio on the orientation density in the X direction

The single specimens showed the highest alignment in the flow direction due to formwork constrictions as expected. The DL specimens obtained by cutting the specimens with a width of 200mm shows greater fiber alignment in the flow direction when compared to TL specimens which were obtained by cutting the specimens with a width of 300mm. Figure 5.4 also shows that the fibers with a length of 6mm are more effectively aligned in the flow direction when compared to the fibers with a length of 13mm. This was expected since these fibers are shorter and their movement is easier when compared to longer fibers.

### 5.1.3. Effect of Specimen Thickness on Fiber Dispersion

Specimen thickness was also expected to be an important parameter since it is a restriction for the fibers that align in the Z direction. Formwork thickness/fiber length (t/fL) parameter is varied by changing the formwork thickness for the fibers with two different lengths.

Figure 5.5 shows variation in the orientation densities in Z direction with an increase in pre-defined t/fL parameter. Alignment of the fibers in the Z direction is found to increase with an increasing thickness of specimens as is seen in Figure 5.5. This parameter is separately evaluated for 2 fibers with different length since fiber dispersion is dominated by various parameters such as mechanical interlocking of fibers which may cause different results.

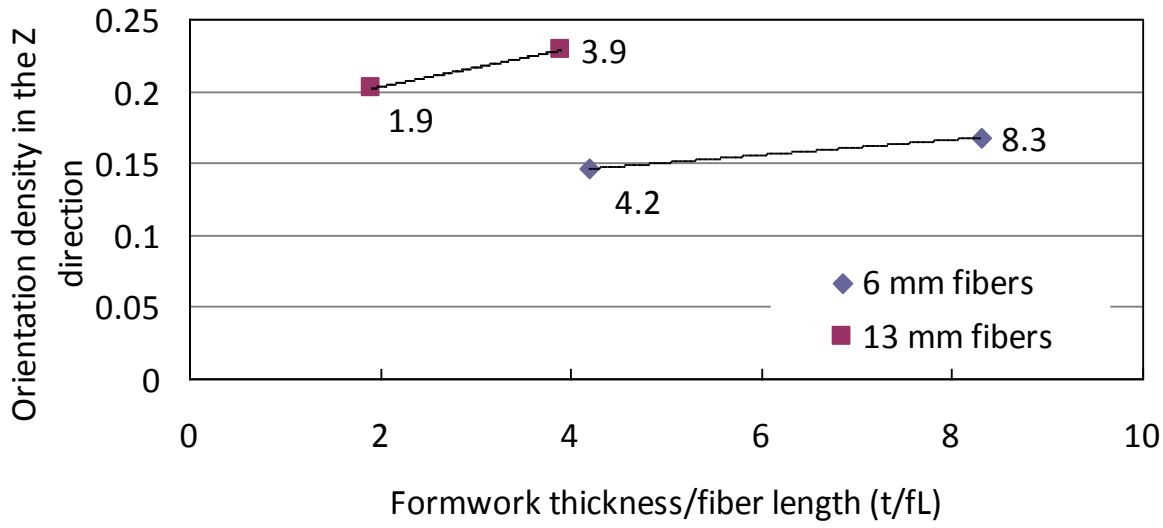


Figure 5.5. Effect of formwork thickness/fiber length ratio on the orientation density in the Z direction

As it can be seen from Figure 5.5, different orientation densities were observed since with a decrease in formwork thickness, hence a decrease in t/fL parameter, fibers tend to align more in casting direction (x-dir.) and less in z-direction. And, with an increase in formwork thickness, hence an increase in t/fL parameter, there will be more space for fibers to freely flow and therefore fibers tend to align more in z-direction.

## 5.2. Segregation Analysis

The most important point in SFRC is obtaining a random dispersion and tailored orientation of fibers. On the other hand, addition of fibers to the SCC may bring up some issues such as static and dynamic segregation of fibers.

Segregation of fibers are related with the viscosity and yield stress of paste, balance between the driving force of the flowing fresh mix due to viscosity, self weight of the fibers, and further by the cross-section shape. Fresh state properties of fiber-reinforced concretes (FRCs) were correlated to hardened state properties by quantifying fiber segregation. Therefore, for a succesful fresh state and hardened state performance, static and dynamic segregation of fibers should be prevented.

### 5.2.1. Static Segregation Resistance

In order to check the static segragation resistance of specimens, cross sections, which were taken before for image analysis were studied. Only Single (S) and Triple Left (TL) specimen cross sections were chosen to be examined for segregation analysis. Number of fibers in the upper part and lower part of these cross sections were counted seperately as seen in Figure 5.6.

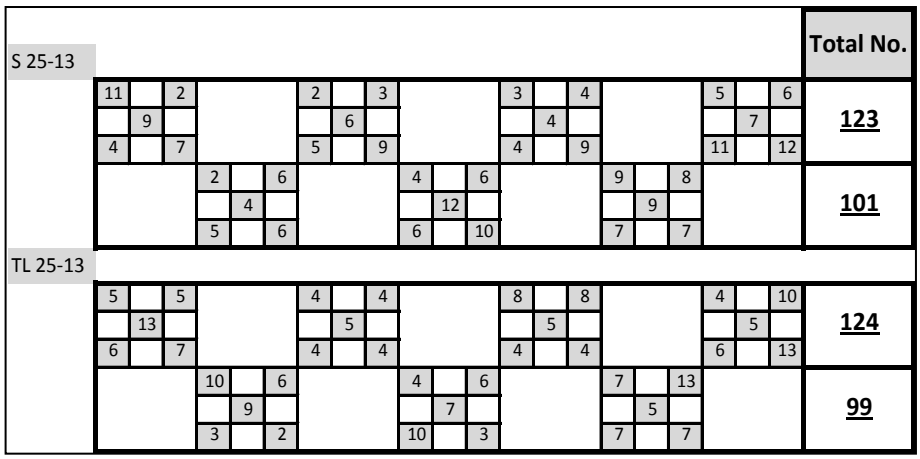


(a)

Figure 5.6. (a) Fiber amounts in each square of S25-13 and TL 25-13 specimens.

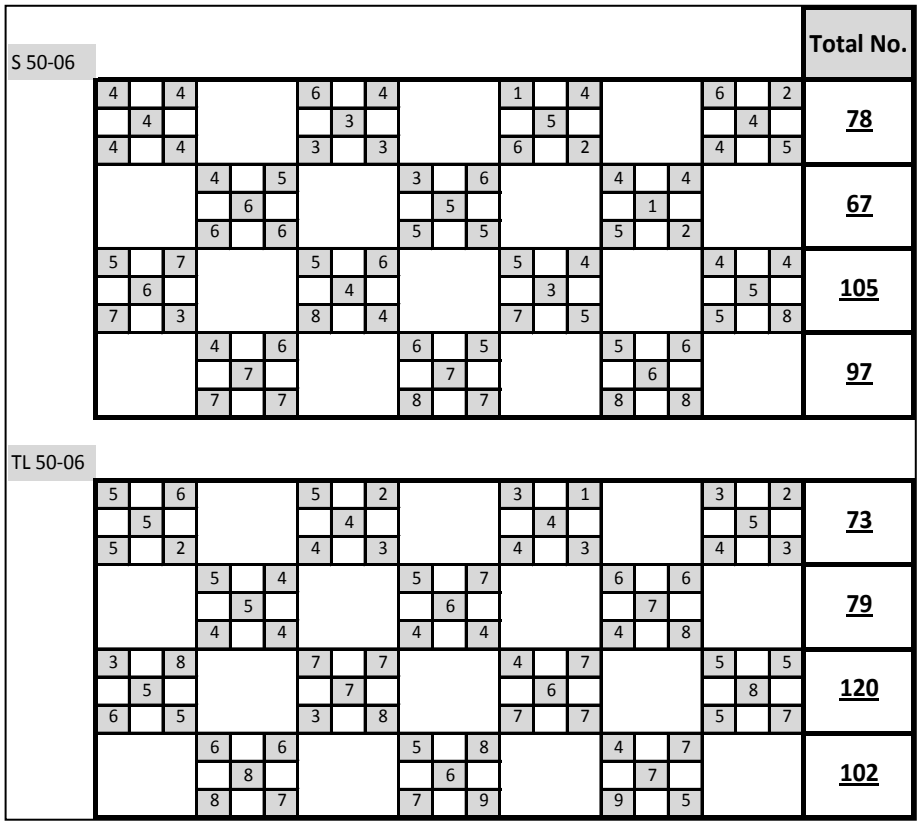


(b)

Figure 5.6. (contd.) (b) Fiber amounts in each square of S50-06 and TL 50-06 specimens.

Calculation of fibers per unit length would be more convenient to make comparison between the segregation resistance of mixes. Therefore, amounts of fiber per unit square (fiber/m²) were calculated seperately for both upper and lower sections of specimens. Furthermore, for more clear understanding of segregation resistance, it would be more convenient to compare the percentages of fibers in both upper and lower parts of the cross sections. (Table 5.2).

Table 5.2. Fiber amounts and percentages of the specimens

| Specimen | Total Fiber | Total Sq. Area | Fiber/UnitArea | Upper Half % Fiber/ Unit Area | Lower Half % Fiber/ Unit Area |
|---|---|---|---|---|---|
| S 25-13 | 123 | 320 | 0,384 | 0,480 | 0,520 |
| | 101 | 240 | 0,421 | | |
| TL 25-13 | 124 | 320 | 0,388 | 0,480 | 0,520 |
| | 99 | 240 | 0,413 | | |
| S 25-06 | 109 | 320 | 0,341 | 0,440 | 0,560 |
| | 103 | 240 | 0,429 | | |
| TL 25-06 | 107 | 320 | 0,334 | 0,420 | 0,580 |
| | 113 | 240 | 0,471 | | |
| S 50-06 | 78 | 320 | 0,244 | 0,420 | 0,580 |
| | 67 | 240 | 0,279 | | |
| | 105 | 320 | 0,328 | | |
| | 97 | 240 | 0,404 | | |
| TL 50-06 | 73 | 320 | 0,228 | 0,410 | 0,590 |
| | 79 | 240 | 0,329 | | |
| | 120 | 320 | 0,375 | | |
| | 102 | 240 | 0,425 | | |
| S 50-13 | 151 | 320 | 0,472 | 0,470 | 0,530 |
| | 148 | 240 | 0,617 | | |
| | 191 | 320 | 0,597 | | |
| | 153 | 240 | 0,638 | | |
| TL 50-13 | 65 | 320 | 0,203 | 0,450 | 0,550 |
| | 75 | 240 | 0,313 | | |
| | 123 | 320 | 0,384 | | |
| | 61 | 240 | 0,254 | | |

It was seen from Table 5.2 when the fiber percentages per unit area were compared, there is very small amount of static segregation in specimens having 25 mm thickness. Specimens having 50 mm thicknesses, showed less resistance to static segregation when compared to 25 mm specimens. Although, there is higher static segregation in thick (50 mm) specimens, these amounts are stil in the allowable limits. Therefore, static segregation of all the specimens are at negligible amounts.

### 5.2.2. Dynamic Segregation Resistance

In order to check the dynamic segragation resistance of specimens, cross sections, which were taken before for image analysis were studied. Single (S) specimen cross sections, having 25 mm thickness were chosen to be examined for segregation analysis.

Cross sections were taken both from middle part and from the end part of the beams, in order to examine how effective is the concrete mixture to drive fibers throughout the mould. Two planes obtained from the middle part (plane 1) and the end part (plane 2) of the beams were examined. Relative positions of the planes are shown in Figure 5.7 below. Plane 2 is obtained 20 mm inside from the end of the mould considering the maximum fiber length (13mm) used for the mixtures.

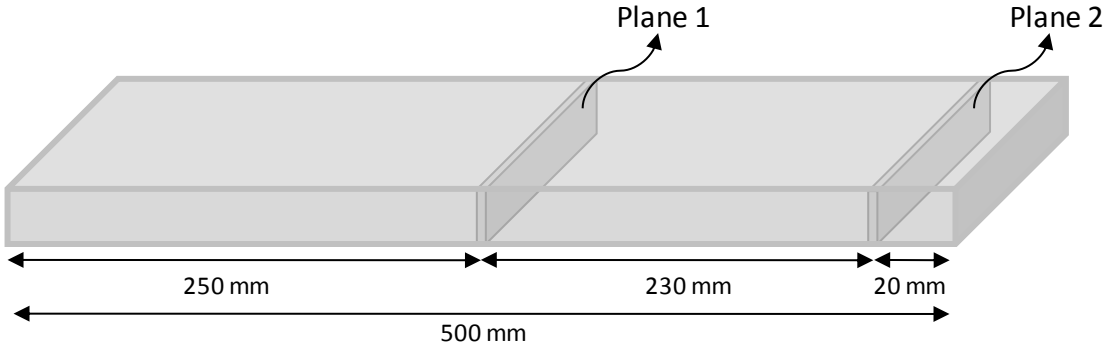


Figure 5.7. Relative positions of the planes, which are examined for dynamic segregation

Table 5.3. Results of Dynamic Segregation Analysis

| Specimen | Number of Fibers | |
|---|---|---|
| | Middle Part | End Part |
| S 25-06 | 1539 | 1287 |
| S 25-13 | 1175 | 1041 |

As is seen in Table 5.3 some dynamic segregation were found in the specimens. However, these values could be considered negligible, since there are very small difference between number of fibers in Plane 1 and number of fibers in Plane 2.

## 5.3. Mechanical Performance

In this work the correlations between toughness properties of SFRC and fiber dispersion related issues, as influenced by the formwork dimensions have been investigated. Therefore, as a final goal of this work the correlation existing between the mechanical performance of the fiber-reinforced composite, as measured through four-point bending tests, and the dispersion of the fibers, as studied through Image Analysis and influenced by the fresh state behavior, has also been tentatively assessed from the quantitative point of view.

### 5.3.1. Load vs. Deflection

As a result of 4-point flexural test it was observed from the Load vs. Deflection curves those 4 groups, each having 6 specimens, showed different behavior as seen in Figure 5.8 (a-d).

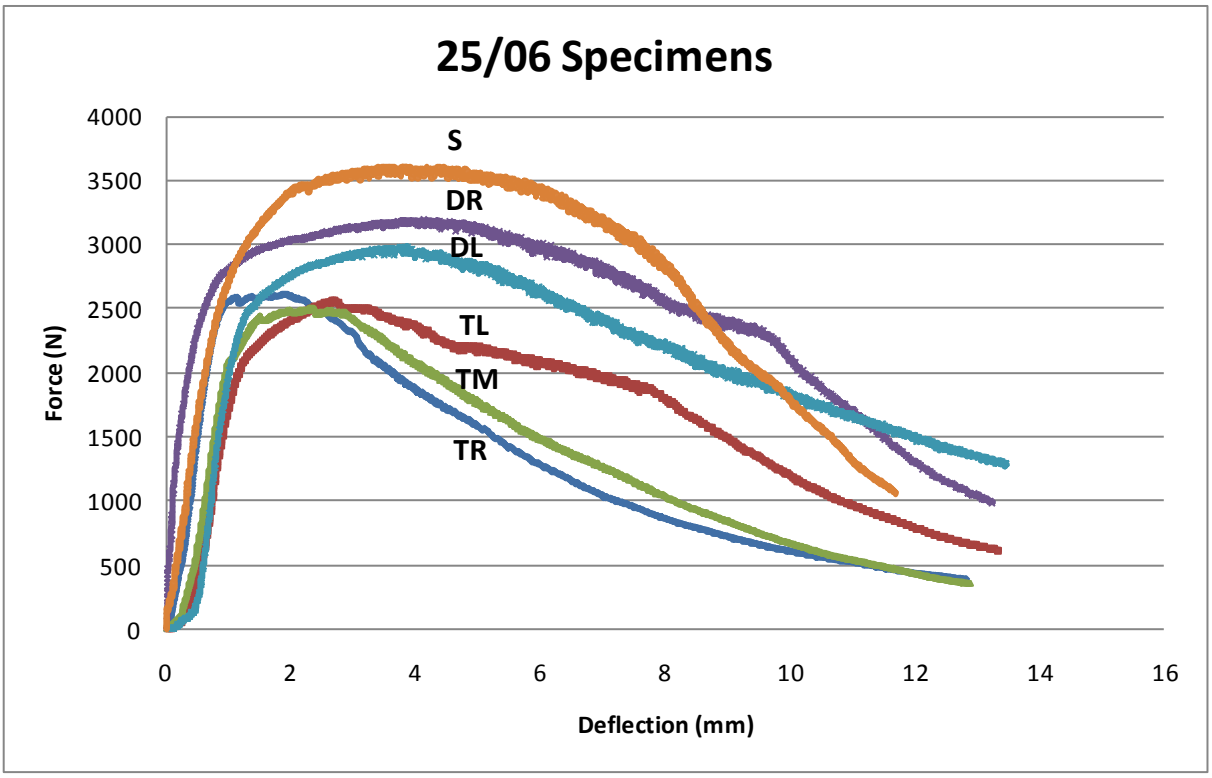


Figure 5.8. (a) Force vs Displacement curves of 25/06

It can be seen from Figure 5.8 (a) that, S, DR and DL specimens showed strain hardening behavior, whereas TL, TM and TR specimens showed strain softening behavior. This difference in the behavior of specimens having same mixture proportions, same fiber content and same thickness is only due to their initial formwork widths, in which casting has been done. Formwork widths of S, DR and DL specimens were less than TL, TM and TR specimens; therefore there was less space for fibers to flow freely in single (S) and double (D) specimen formworks. This flow constraint caused nearly 1D flow in single (S) and double (D) specimens, therefore fibers aligned in casting direction (x-dir) were more than that of triple (T) specimens. As seen from Table 5.1, fiber orientation density (FOD) of S 25-06 specimen is the highest (0,703) and following this DL (0,672), which is slightly less than single (S) specimen and finally TL and TM having nearly the same FOD (0,66) in the x-direction. This makes sense that S specimen having the highest FOD in casting direction, since single moulds have the least width and hence more restriction on the flow, forcing it to be nearly 1D. As a result of this difference in alignment, specimens having more fibers aligned in the casting direction had more control on crack formation by better bridging cracks. Hence, sudden formation of larger cracks were prevented and specimens showed more ductility compared to ones having less fibers aligned in the casting direction.

In addition to that, again due to the fiber orientation densities in casting direction, maximum load beared by S 25-06 is the highest of them all, and then comes sequentially DR 25-06, DL 25-06, TL 25-06, TM 25-06, and TR 25-06. This was expected, since S 25-06 has the highest FOD in casting direction, which caused higher flexural strength, compared with the specimens having less FOD in the casting direction.

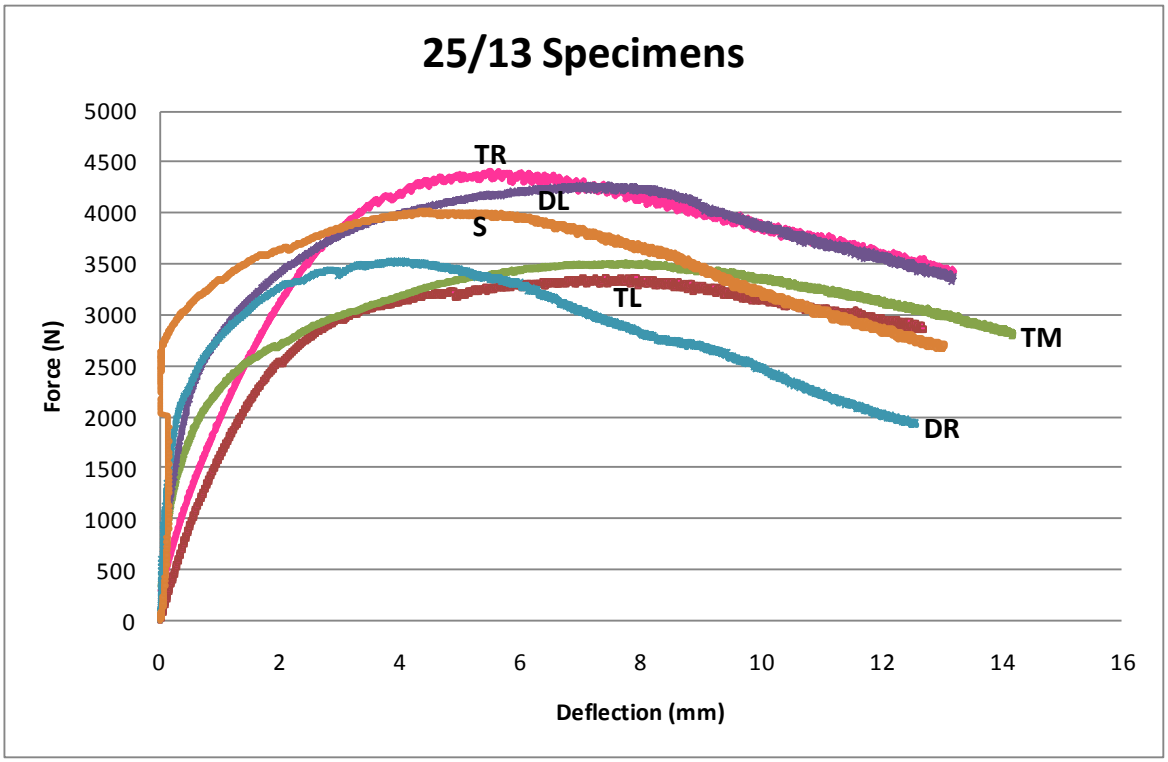


Figure 5.8. (b) Force vs Displacement curves of 25/13

It can be seen from Figure 5.8 (b) that, all of the specimens of group 25-13 showed strain hardening behavior. Compared with specimens of 25-06 group, the only difference of 25-13 group is fiber length, apart from that mixture proportions, fiber content and formwork thicknesses are all the same. Only S, DR and DL specimens showed strain hardening behavior with 6 mm long fibers, but with 13 mm long fibers all groups of specimens showed strain hardening behavior. This difference in fiber length caused the different behavior of specimens due to the increased load bearing capacity with increased aspect ratio of fibers. As the aspect ratio of fibers increased, the risk of pulling out of fibers from the concrete matrix decreases. Therefore, ductility and toughness of the specimens increases.

The differences in the behavior of same group of 25-13 specimens having same mixture proportions, fiber content and thickness is also due to their initial formwork widths. Flow constraint in moulds, caused nearly 1D flow in single (S) and double (D) specimens, therefore fibers aligned in casting direction (x-dir) were more than that of triple (T) specimens. As seen from Table 5.1, fiber orientation density (FOD) of DL 25-06 specimen is the highest (0,588) and following this S (0,568), which is slightly less than

single (DL) specimen and finally TL having (0,496), TM having (0,562) FOD in the x-direction. DL has the highest FOD in casting direction for 25-13 group specimens. As a result of this difference in alignment, specimens having more fibers aligned in casting direction had more control on crack formation by bridging cracks better. Hence specimens showed more ductility compared to ones having less fibers aligned in the casting direction.

For 25-13 group specimens, the maximum load is beared by TR 25-13, compared to single (S) and double (D) specimens. However, S 25-13 was expected to have the highest maximum load. This may be due to the FOD of TR 25-13 in casting direction. But, TR 25-13 FOD wasn't calculated, since it was expected to be nearly the same as the TL 25-13 due to symmetry. Although, maximum load of S 25-13 is less than that of TR 25-13 and DL 25-13, still it has higher Young's Modulus (hence being more stiff) and it is more ductile than TR and DL specimens.

Another difference between the Force-Displacement curves of 25-06 and 25-13 specimens, is that maximum load beared by all of the 25-13 specimens are higher than that of 25-06 specimens. As it was seen in Figure 5.8 (a) that, maximum load of S 25-06 specimen was about 3600 N, whereas maximum load of S 25-13 specimen was nearly 4400N. It can be said that increased fiber length, made FRC specimens more resistant to flexural strength, since fiber aspect ratio has increased. As it was also stated in the study of Yazıcı et al.[49], flexural strength of SFRC is significantly improved with increasing aspect ratio (l/d).

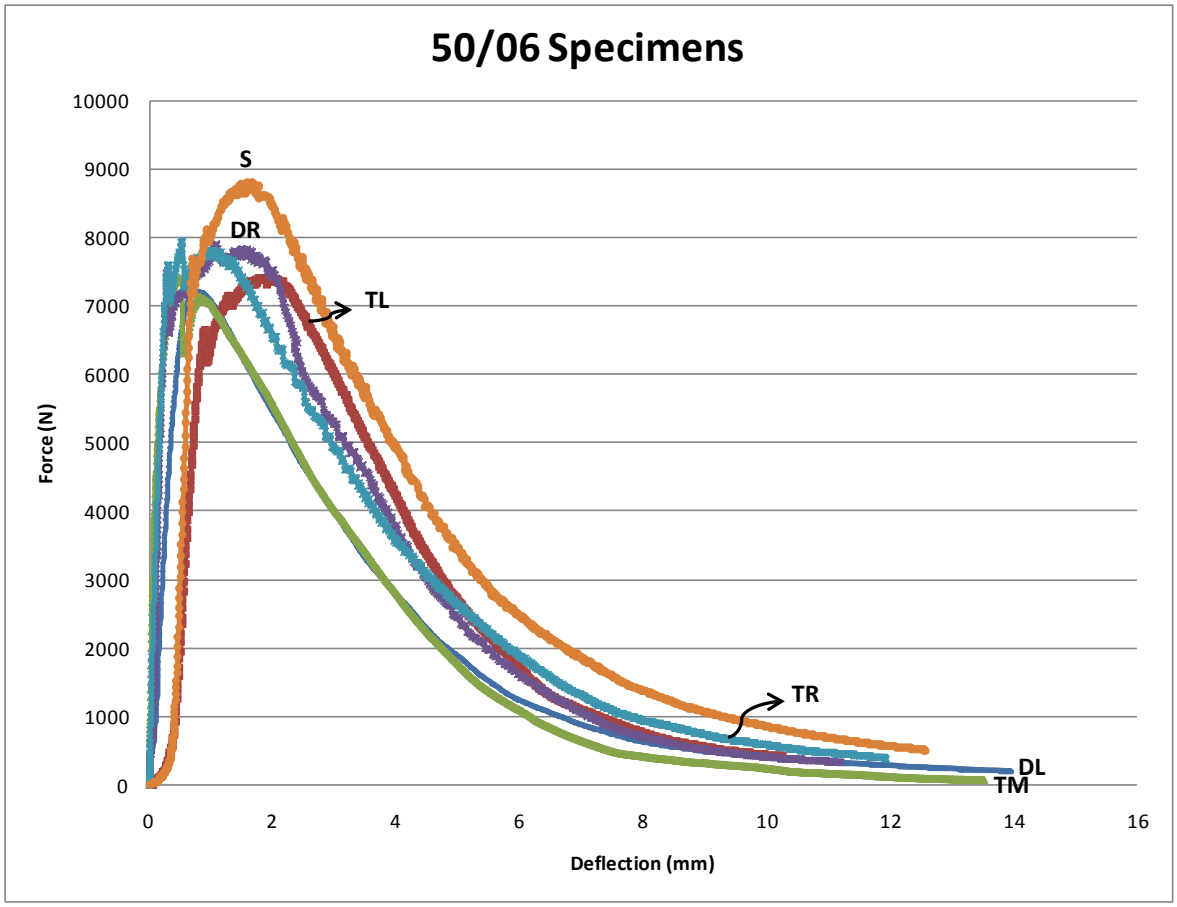


Figure 5.8. (c) Force vs Displacement curves of 50/06

Since these graphs are showing only Force-Displacement relationship, specimen groups having 25 mm and 50 mm thickness will be compared independently. As it was seen from Figure 5.8 (c) that, all of the specimens of group 50-06 showed strain softening behavior.

The differences in the maximum load of 50-06 specimens having same properties are due to their initial formwork widths, as mentioned before. All specimens showed similar behavior. Flexural toughness parameter will be used to evaluate ductility of different specimens. S 50-06 again beared the highest load. This result is also confirmed by FOD values, S specimen having 0,707 and DL, TL, and TM having FOD values respectively, 0,664, 0,618 and 0,626, which are very close to each other.

Therefore, again due to the differences in formwork widths, hence due to FOD in casting direction, maximum load beared by S 50-06 is the highest of them all, and then comes sequentially DR 50-06, DL 50-06, TL 50-06, TM 50-06, and TR 50-06.

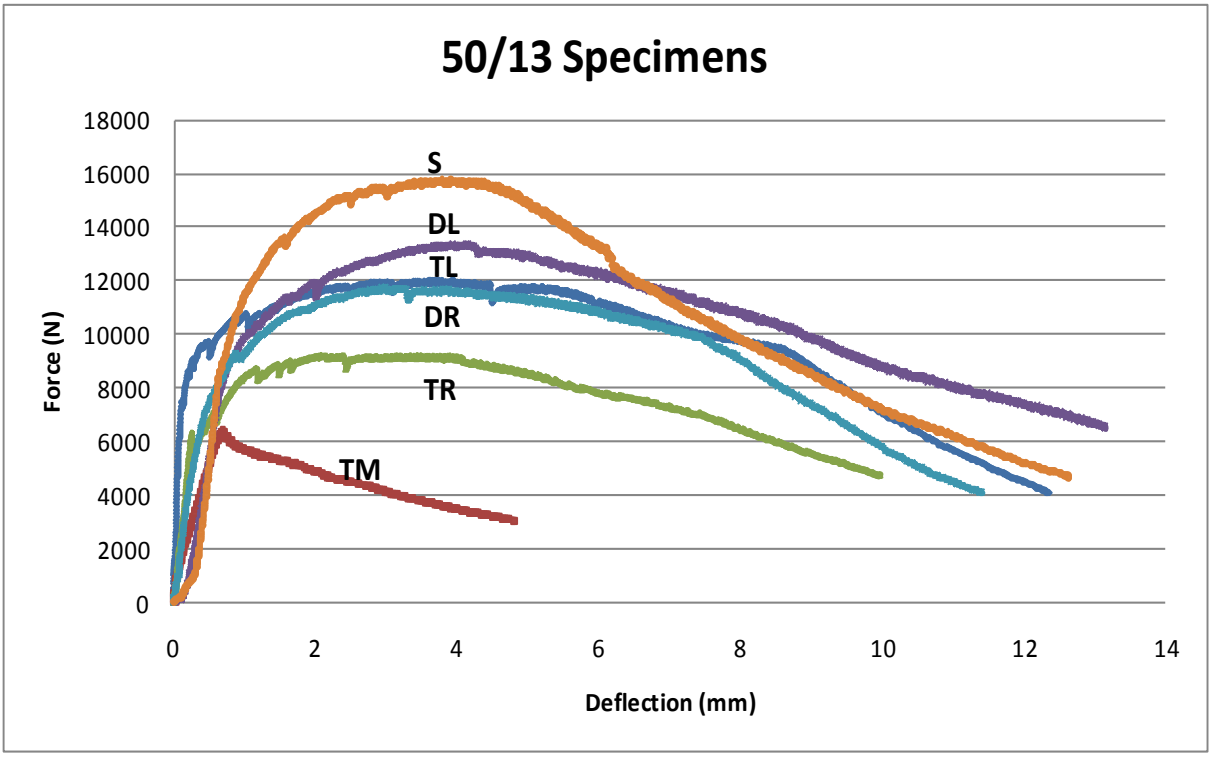


Figure 5.8. (d) Force vs Displacement curves of 50/13

It can be seen from Figure 5.8 (d) that except TM 50-13 specimen, all of the specimens of 50-13 group showed strain hardening behavior. The difference in the behavior of TM 50-13 specimen is due to a pre-loading error occured during the experiment. It was seen from the figure that again, single (S) specimen bears the highest load, when compared to the double (DR, DL) and triple (TR, TM, TL) specimens.

As seen from Table 5.1, fiber orientation density (FOD) of S 25-06 specimen is the highest (0,632) and DL, TL and TM specimens have the following FOD values, respectively (0,601- 0,547- 0,551).

These results imply the important relation between fiber orientation and flexural strength. It also shows the ability of image analysis to represent fiber dispersion state in the specimen.

Comparison between Force-Displacement curves of 50-06 and 50-13 specimens, shows that at maximum load beared by all of the 50-13 specimens are higher than that of 50-06 specimens. As it was seen in Figure 5.8 (c-d), maximum load of S 50-06 specimen was about 8800 N, whereas maximum load of S 50-13 specimen was nearly 16000N. This difference between the maximum loads beared by the specimens are due to the fact that, increased fiber length, made FRC specimens more resistant as it was mentioned by various researchers.

### 5.3.2. Load vs. Crack Opening Displacement (COD)

Load-COD behavior of specimens are related with the effectiveness of the fresh concrete to align fibers along the flow direction due to its viscosity. In addition to that, they give information about the relationship between fiber orientation results and mechanical performance of the specimens in the hardened state. The concrete flow in Single (S) specimens were nearly 1D flow, since they have both narrow thickness and width. Therefore, it was expected that the flow will be more parallel to the long sides of the moulds, when compared with the double (D) and triple (T) specimens. Load-COD behavior of all group specimens are shown in the Figure 5.9 (a-c):

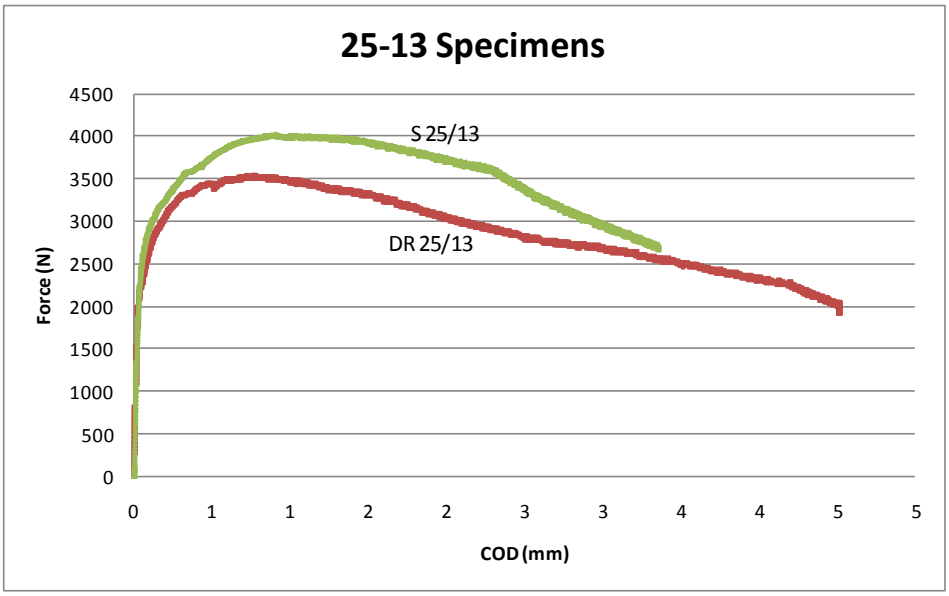


(a)

Figure 5.9. (a) Graph, showing relationship between Force and Crack Opening Displacement (COD) of the 25-13 specimens

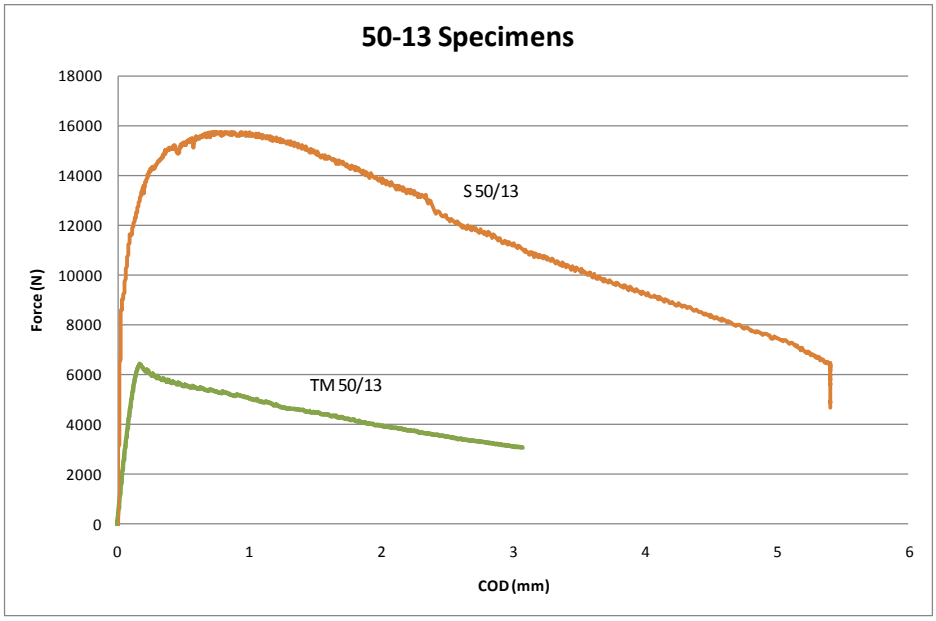


(b)

Figure 5.9. (b) Graph, showing relationship between Force and Crack Opening Displacement (COD) of the 50-13 specimens

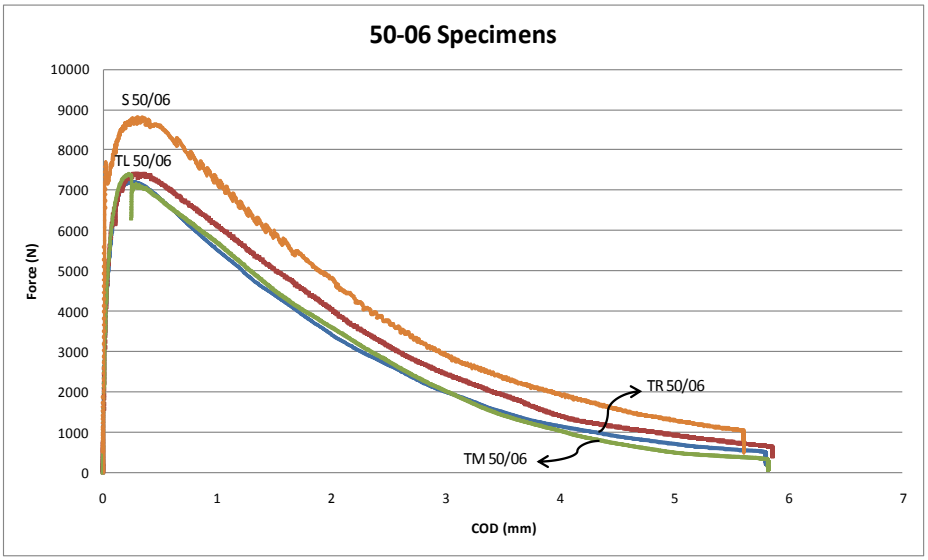


(c)

Figure 5.9. (c) Graph, showing relationship between Force and Crack Opening Displacement (COD) of the 50-06 specimens

Load-COD relation could not be obtained for all the specimens since crack occurred out of the LVDT measurement range for some of the specimens. As is seen from Figure 5.9 (a-c) Force-COD curves are obtained for some specimens of 25-13, 50-13 and 50-06 groups.

In Figure 5.9 (a), it can be seen that S 25-13 beared more load compared to DR 25-13, before failure observed. Therefore, more force is needed for S 25-13 sepcimen to observe the same amount of crack opening displacement as DR 25-13.

It can be seen that, S 50-13 specimen resist much more load compared to TM 50-13 specimen, in Figure 5.9 (b). As a result, for the same amount of crack opening, more force is needed for S 50-13 specimen. For 50-06 specimens, as seen in Figure 5.9 (c), again single (S) specimen bears the highest load compared to TL, TM and TR specimens.

These different Load-COD behavior of the specimens are again due to different fiber orientation densities (FOD). Since, single (S) specimens had higher FOD in the casting direction (x-dir) they had more control on crack formation and propogation by better bridging cracks. As a result, they have more resistance on the cracks to propogate and single (S) specimens undergo higher loads before observing the same crack opening displacement, compared to ones having less fibers aligned in the casting direction.

### 5.3.3. Flexural Strength ($F_{net}$)

The addition of fibers leads to improvements in ductility, toughness, and flexural strength [11],[50]. From the bending tests flexural strengths were determined, with the following $F_{net}$ formula:

$$F_{net} = \frac{3\,PL}{2B\,(D-a_o)^2} \tag{7}$$

where $F_{net}$ is flexural strength (N/mm²), P is the fracture load (N), L is the distance between the supports (mm), B is the width of the specimen (mm), D is the depth of the specimen (mm) and $a_o$ is the notch depth (mm). For $F_{net}$calculations in present study, $a_o$ is taken as zero, since loading was applied to unnotched beams.

Previously, it was mentioned that two parameters were defined to understand the effects of varying formwork dimensions on the fiber alignment and resulting mechanical performance. One of the parameters was selected to be the ratio of formwork width to the fiber length (w/fL) and the other one was the ratio of formwork thickness to the fiber length (t/fL). Therefore, in order to determine the relationship between formwork dimensions and mechanical performance clearly, it is needed to consider formwork width and formwork thickness separately.

5.3.3.1. Relationship Between (w/fL) Parameter and Flexural Strength: For all group of concrete mixtures, one of the variables were formwork width, whereas mixture proportions, fiber content and formwork thickness kept constant. Therefore, different flow behaviors were expected since with a decrease in formwork width, there would be less space for material to flow freely and with an increase in formwork width there would be more space for material to flow freely. This flow width constraint caused nearly 1D flow in single (S) and double (D) specimens, and as a result, steel fibers aligned in casting direction (x-dir) more than that of triple (T) specimens. Therefore, different alignment of fibers in casting direction caused some differences in the mechanical performance of specimens, which are casted to moulds having different widths.

For better understanding of the relationship between formwork width and mechanical performance, a parameter relating formwork width to fiber length (w/fL) were determined. For 6 mm fibers, this w/fL parameter is set to be 16.7, 33.3 and 50 respectively for single (S), double (D) and triple (T) specimens. And, for 13 mm fibers it is 7.7, 15.4 and 23.2 respectively for single (S), double (D) and triple (T) specimens. In Figure 5.10 (a) and (b) the relationship between w/fL and flexural strength can be seen.

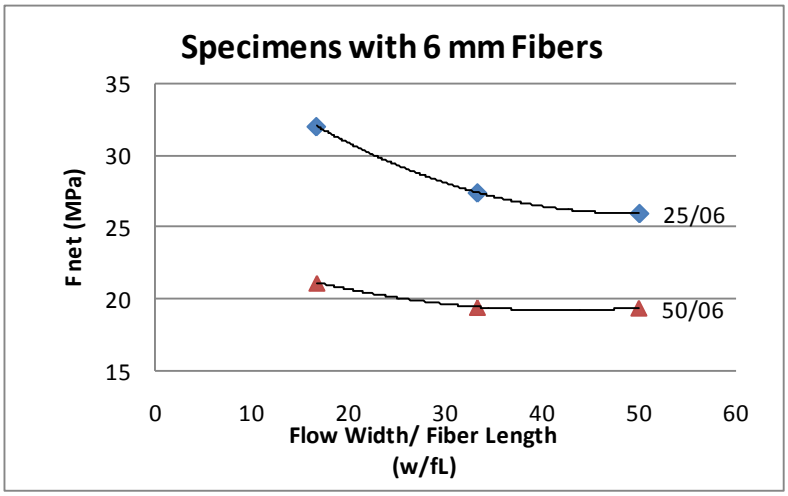


(a)

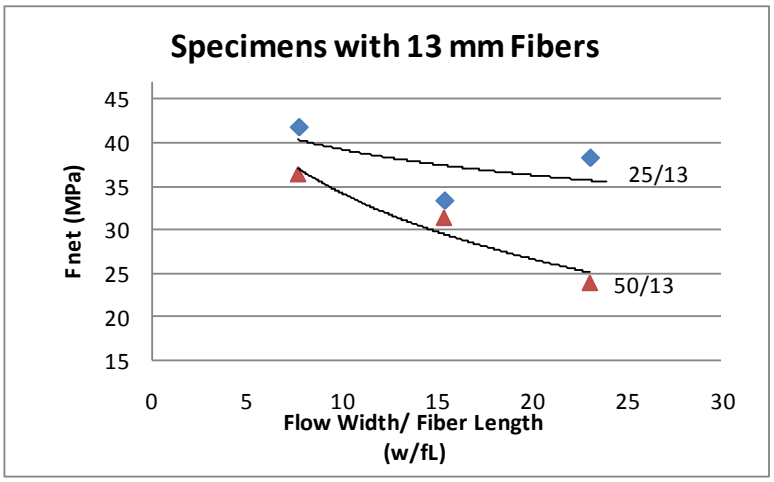


(b)

Figure 5.10. (a-b) Graphs, showing relationship between Flexural Strength and (w/fL) parameter

As it is seen from Figure 5.10 (a) and (b) that flexural strength is dependent on formwork width. Flexural toughness of specimens decreases with an increase in the w/fL parameter for all of the groups. Considering specimens with 6 mm fibers, for beams with 25 mm thickness, an increase in w/fL parameter causes a greater decrease in flexural strength, compared with the ones having 50 mm thickness. On the other hand, considering specimens with 13 mm fibers, for beams with 50 mm thickness, an increase in w/fL parameter causes a greater decrease in flexural strength, compared with the ones having 25 mm thickness. Therefore, flexural strength of thin specimens having fibers with smaller aspect ratio and thick specimens having fibers with higher aspect ratio are more affected by flow width.

5.3.3.2. Relationship Between (t/fL) Parameter and Flexural Strength**:** As it was mentioned before, for all group of concrete mixtures, another variable was formwork thickness, whereas mixture proportions, fiber content and formwork width kept constant. Therefore, different flow behaviors were expected since with a decrease in formwork thickness, fibers tend to align more in casting direction (x-dir.), but with an increase in formwork thickness, there will be more space for fibers to freely flow and therefore fibers tend to align in all directions. Hence a decrease of the fiber alignment in x-direction and an increase of the fiber alignment in z-direction is expected.

For better understanding of the relationship between formwork thickness and mechanical performance, a parameter relating formwork thickness to fiber length (t/fL) were determined. For 6 mm fibers, t/fL parameter is 4.2 and 8.3 respectively for 25 mm and 50 mm specimens. And, for 13 mm fibers it is 1.9 and 3.9 respectively for 25 mm and 50 mm specimens. In Figure 5.11 (a-f) the relationship between t/fL and flexural strength ($F_{net}$)can be seen.

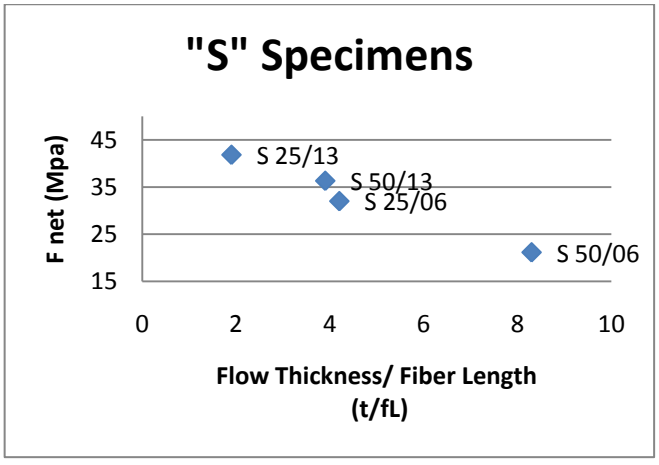


(a)

Figure 5 .11. (a) Graph, showing the relationship between Flexural Strength ($F_{net}$) and Flow Thickness/ Fiber Length (t/fL) parameter for S groups

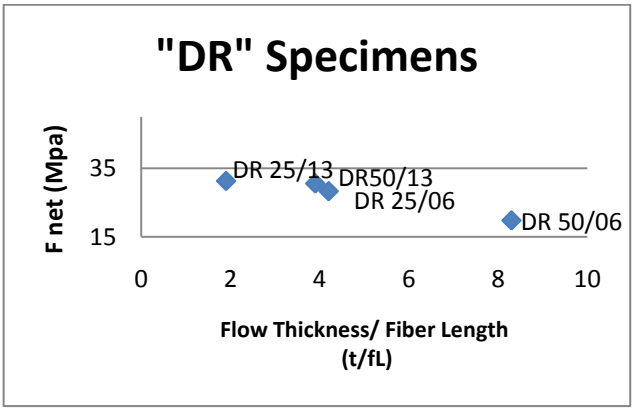


(b)

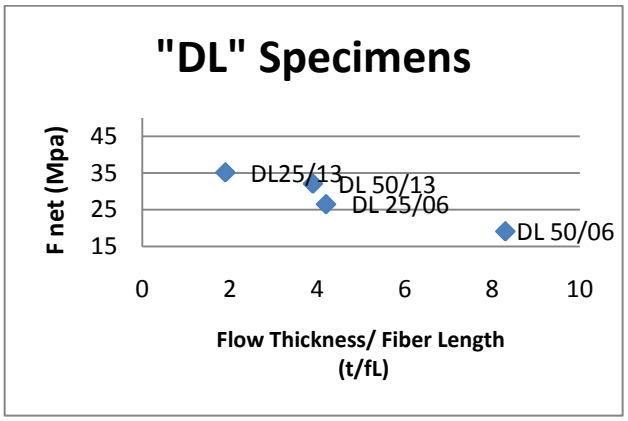


(c)

Figure 5 .11. (contd.) (b-c) Graphs, showing the relationship between Flexural Strength ($F_{net}$) and Flow Thickness/ Fiber Length (t/fL) parameter for DR and DL groups

As it is seen from Figure 5.11 (a-c) single and double specimens made with 13 mm fibers have higher flexural strengths when compared to the specimens made with 6 mm fibers.

For all groups of single and double specimens, an increase in t/fL parameter decreases flexural strength. Considering specimens with 13 mm fibers, an increase in t/fL parameter causes less decrease in flexural strength, when compared to specimens with 6 mm fibers. From this result it can be concluded that, short fibers are more affected by the changes in flow thickness.

Only exception to that are seen when TR and TM specimens were examined. Flexural strength of TR 25/06 and TM 25/06 are found to be greater than TR 50/13 and TM 50/13.

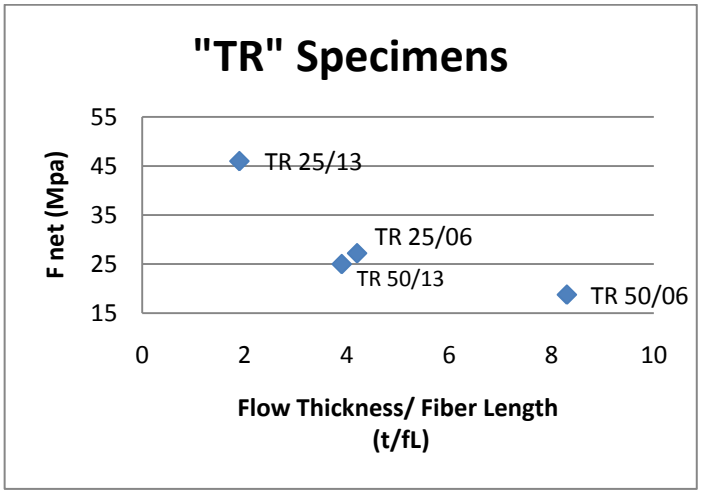


(d)

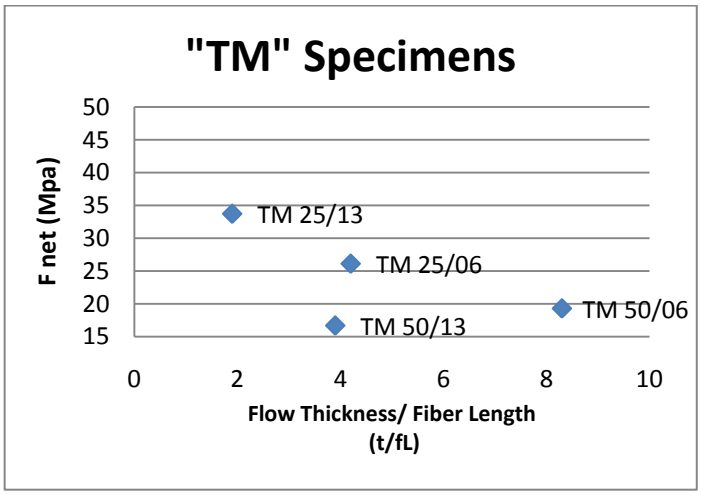


(e)

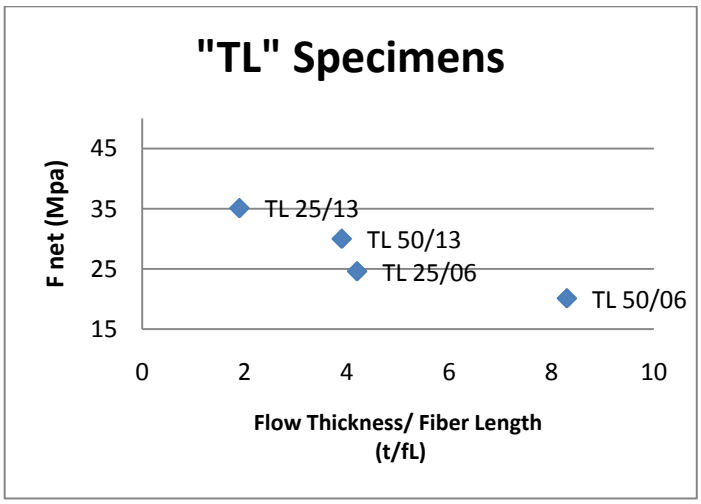


(f)

Figure 5.11. (contd.) (d-f) Graphs, showing the relationship between Flexural Strength ($F_{net}$) and Flow Thickness/ Fiber Length (t/fL) parameter for TR, TM and TL groups

As it is seen from Figure 5.11 (d-f) that for triple (T) specimens with 13 mm fibers, don't have higher flexural strengths in all cases, when compared with the specimens having 6 mm fibers. This can be due to the differences in fiber orientation density (FOD). Because, triple (T) specimens have more flow width while casting, compared to S and D specimens; therefore, they have less FOD in the casting direction. As a result of increase in flow thickness, a decrease in FOD in casting (x) direction and an increase in FOD in z-direction is observed, since there are more free space for fibers to rotate and align in z-direction.

Table 5.4. FOD of triple (T) specimens in the z-direction

| **Specimen** | **FOD in z-direction** |
|---|---|
| TL 25-06 | 0,156 |
| TM 25-06 | 0,163 |
| TL 50-06 | 0,183 |
| TM 50-06 | 0,177 |
| TL 25-13 | 0,193 |
| TM 25-13 | 0,214 |
| TL 50-13 | 0,247 |
| TM 50-13 | 0,215 |

As it was shown in Table 5.4, triple specimens with same fiber aspect ratios having 50 mm thickness have more fibers oriented in z-direction compared with the specimens having 25 mm thickness. Therefore, as it was seen from Figure 5.11 (d-f) that specimens with 50 mm thickness have less toughness strength, since they have more fibers oriented in the z-direction and less fibers oriented in the x-direction, compared with the specimens having 25 mm thickness. As a result, FOD in the z-direction increases, when thickness is increased from 25 to 50 mm and that leads to higher $F_{net}$ values for the specimens with a higher thickness.

### 5.3.4. Flexural Toughness

The toughness of fiber-reinforced concrete (FRC) materials can be considered as their energy absorption capacity, which is usually characterised by some portion of the area under the load-displacement curve obtained during a flexure test. [51] Most toughness measurements have been performed on un-notched beams in flexure using a four-point loading arrangement.

The most common method to measure toughness is to use the load-deflection curve obtained using a simply supported beam loaded from four points (four-point bending) [52]. The two widely used standard test methods are the ASTM C 1018 standard test method and the Japan Society of Civil Engineerrs (JSCE) standard SF-4 method. In this study, JSCE SF-4 method was used for flexure toughness calculations. The JSCE SF-4 equation used for flexural toughness calculations is as following in Eqn.5:

$$FT = \frac{A_{(L/150)} \cdot L}{(L/150) b h^2} \tag{8}$$

where, FT is the flexural toughness (MPa), A is the area under Load-Deflection curve (N.mm), L is the distance between supports (mm), b is the width of the beams (mm) and h is the thickness of the beams (mm).

In this study, since end point deflection values for specimens were about 10 mm, $A_{(L/150)}$ value was taken as the area under the load vs. deflection curve upto 10 mm deflection.

JSCE flexural toughness (FT) at a deflection $\delta$ = 10mm were calculated for all the specimens as explained in 4.2 and results are evaluated by means of the two parameters defined in the beginning of the project.

5.3.4.1. Relationship between (w/fL) parameter and Flexural Toughness: As it can be seen from Figure 5.12 (a) and (b) that flexural toughness of specimens decreases with an increase in the w/fL parameter for all the groups as expected. This is due to decreased alignment in the casting direction with an increase in the formwork width as shown in

Table 5.1 and Figure 5.4. It is clearly seen that flexural toughness is dependent on formwork dimensions.

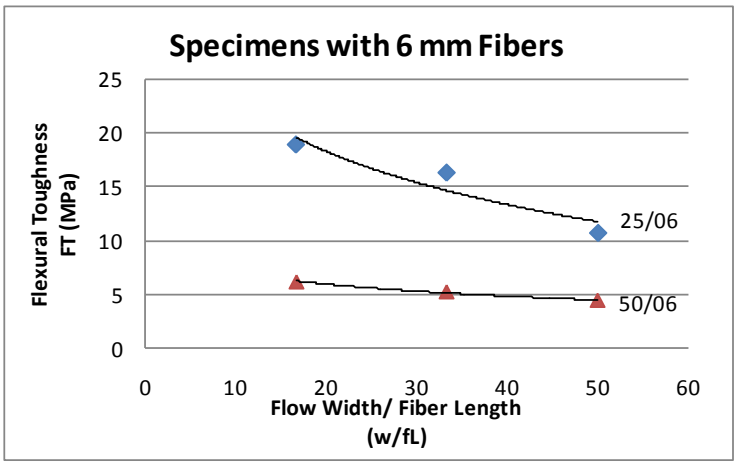


(a)

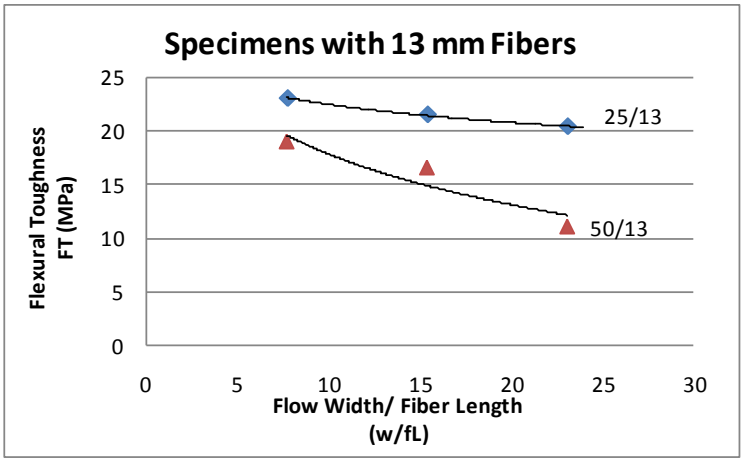


(b)

Figure 5.12. (a), (b) Relationship between w/fL parameter and flexural toughness

5.3.4.2. Relationship between (t/fL) parameter and Flexural Toughness: Formwork thickness also creates a constriction for the fibers and effects their alignment. Evaluation of t/fL parameter clearly shows in the Figure 5.13. (a-d) that flexural toughness of groups of specimens decreases when t/fL increases.

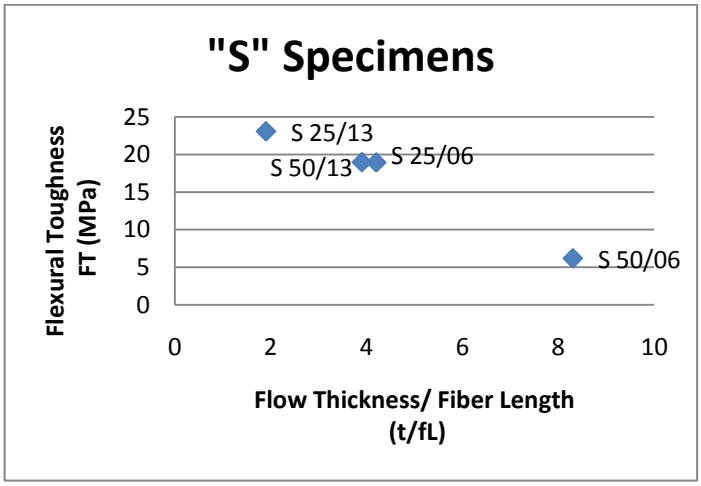


(a)

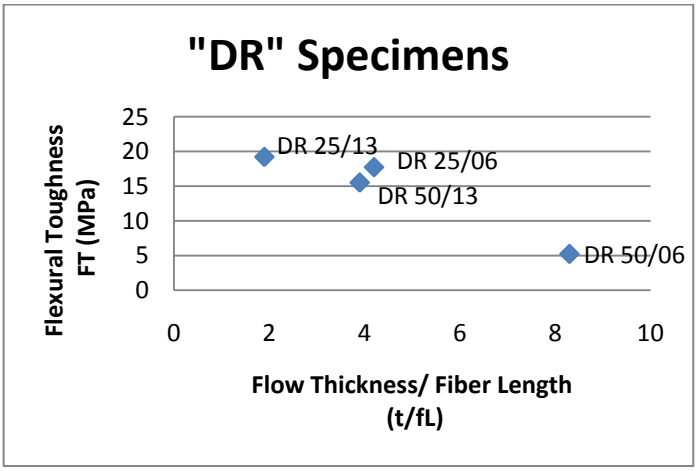


(b)

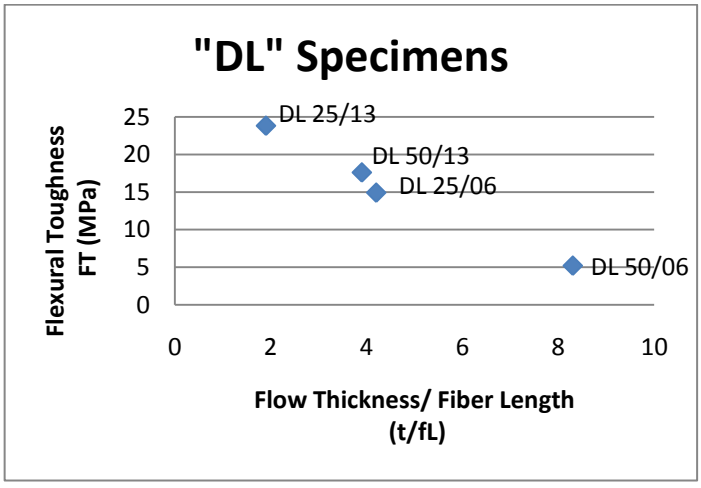


(c)

Figure 5.13. (a-c) Relationship between Flexural Toughness (FT) and Flow Thickness/ Fiber Length (t/fL) parameter for S, DR and DL groups

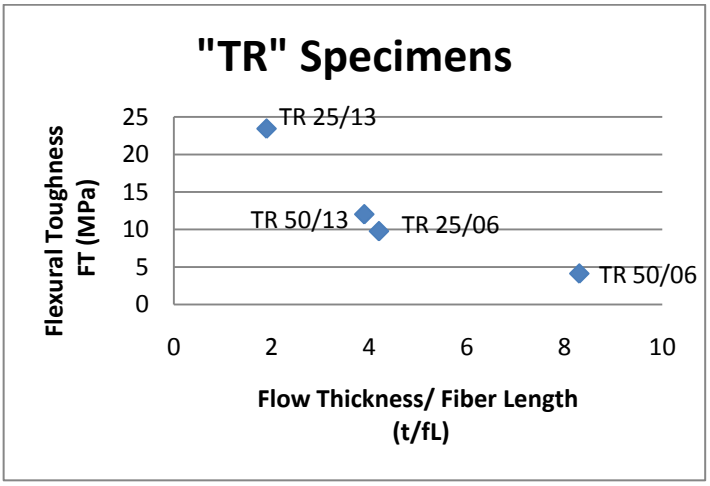


(d)

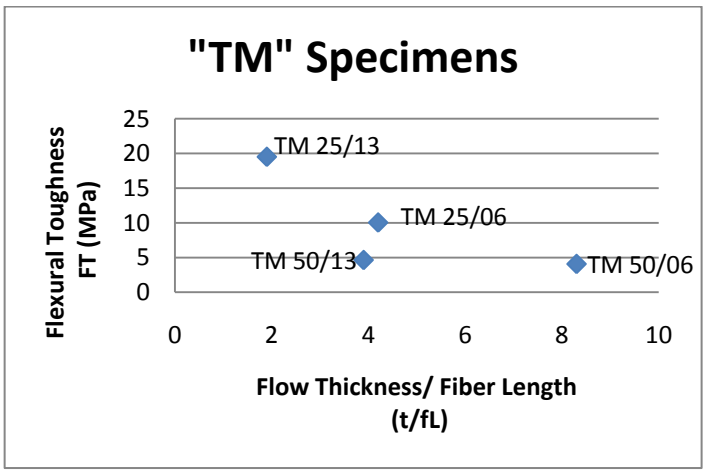


(e)

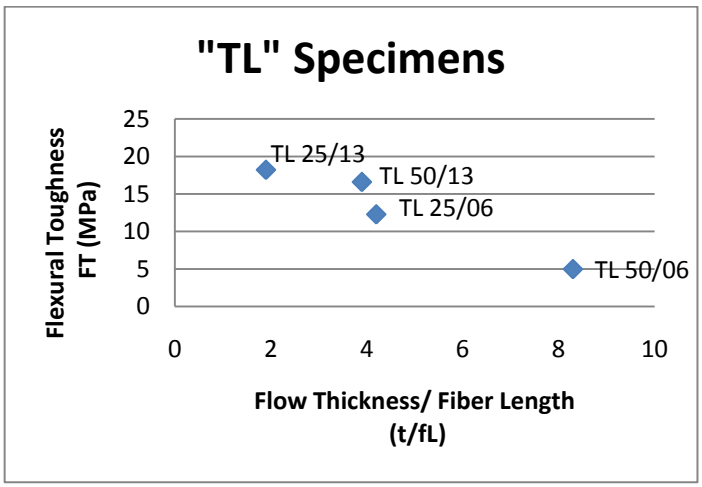


(f)

Figure 5.13. (contd.) (c-f) Relationship between Flexural Toughness (FT) and Flow Thickness/ Fiber Length (t/fL) parameter for TR, TM and TL groups

Increased t/fL means lower numbers of aligned fibers in the flow direction and this result in less number of fibers which will work to arrest cracks. This result could also be confirmed by using the results of image analysis (Figure 5.5). Orientation density in the Z direction decreases when t/fL value decreases and this means greater orientation density in the XY plane with a greater flexural toughness as a result.

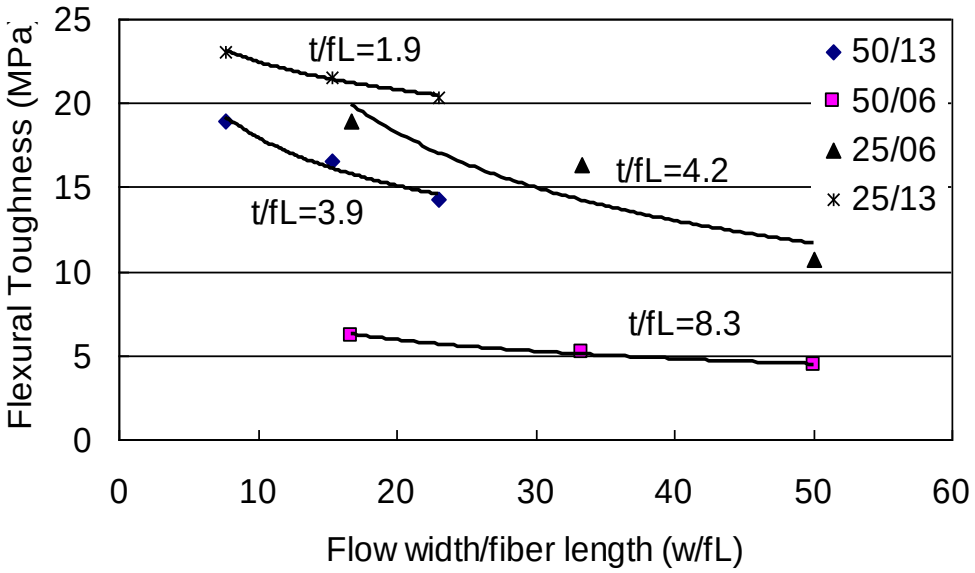


Figure 5.14. Effect of w/fL and t/fL on the flexural toughness of specimens

# 6. CONCLUSIONS

The main objective of this study was to investigate the effects of formwork dimensions/mould constraints on the fiber dispersion features and resulting mechanical performance. For this purpose, two parameters were defined (w/fL and t/fL) and following results were drawn as a result of experimental study:

- Short-cut steel fibers have a tendency to align in the flow direction.
- Formwork walls act as barriers and constrict fibers as well as material.
- If there is more space for the material to spread in the formwork, fibers also spread in the plane instead of being aligned in the casting direction. Alignment in the casting direction decreases with an increasing formwork width. Short fibers better flow with the material and align themselves in the direction of the flow. Ability of long fibers to align themselves in the direction of flow was found to be less than short fibers, probably due to mechanical entanglement.
- Alignment in the Z direction increases when the ratio of formwork thickness/fiber length increases. This is expected considering that the fibers have more free space to move inside the formwork with an increasing thickness.
- In general, different dispersion characteristics are desired for different applications: while a 1-D alignment could be beneficial for a tensile or bent member which will bear loads in only 1 direction, random alignment (in three directions) of fibers would be necessary for a member which will meet forces from two (i.e. a slab) or 3 directions. This study focus on beam specimens and the alignment of fibers in the XY plane and especially in the X direction increases the probability of hitting fibers through the main crack path resulting in greater resistance to opening of cracks. These results show that mechanical performance of the materials could be increased to an important extent if a proper design observing requirements of the application is done.
- The strength of a structure made of fibre reinforced concrete is dependent of the fibre alignment and fibre distribution, which both can be influenced by the properties of fresh concrete.

- Flexural toughness of the specimens decreases with an increasing w/fL value. Formwork thickness/fiber length parameter was also found to be effective on the flexural toughness values, FT decreasing with an increase in t/fL.

Results of this experimental study show the extent to which the formwork dimensions/restrictions affect fiber dispersion features and resulting mechanical performance.

Remarkable variations were seen in FT values when the two parameters were varied. These results emphasize the importance of considering the effects of the parameters such as the ratio of formwork width/fiber dimension and formwork thickness/fiber dimension in the fiber-reinforced cement-based materials design procedure.

# REFERENCES


1. Mobasher, B. and S.P. Shah, "Test Parameters in Toughness Evaluation of Glass Fiber Reinforced Concrete Panels", *ACI Materials Journal*, pp. 448-458, Sept-Oct. 1989.

2. Mobasher, B. and C.Y. Li, "Mechanical Properties of Hybrid Cement Based Composites", *ACI Materials Journal*, Vol. 93, No. 3, pp. 284-293, 1996.

3. Oh BH. "Closure to Flexural Analysis of Reinforced Concrete Beams Containing Steel Fibers", *Journal of Structural Engineering*, Vol. 120, No. 6, 1994.

4. Campione G and M.L. Mangiavillano, "Fibrous Reinforced Concrete Beams in Flexure: Experimental Investigation, Analytical Modeling and Design Considerations", *Engineering Structures*, Vol. 30, No. 11, pp. 2970-2980, 2008.

5. Lim D.H. and B.H. Oh, "Experimental Investigation on the Shear of Steel Fibre Reinforced Concrete Beams", *Engineering Structures*, Vol. 21, No. 10, pp. 937-944, 1999.

6. Chunxiang Q. and I. Patnaikuni, "Properties of High-Strength Steel Fiber-Reinforced Concrete Beams in Bending", *Cement and Concrete Composites*, Vol. 21, No. 1, pp. 73-81, 1999.

7. Shah, S.P. and K.G. Kuder, "Hybrid and High Performance Fiber Reinforced Cementitious Composites", *Proceedings of the International Workshop on Advances in Fiber Reinforced Concrete*, Bergamo, Italy, pp. 83-92.

8. Romualdi J.P. and G.B. Batson GB, "Mechanics of Crack Arrest in Concrete", *Proceedings of ASCE*, Vol. 89, No. 3, pp. 147–68, 1963

9. Mobasher B. and C.Y. Li, "Effect of Interfacial Properties on the Crack Propagation in Cementitious Composites", *Advanced Cement Based Materials*, Vol. 4, No. 3–4, pp. 93–105, 1996

10. Nawy E.G., *Fundamentals of High-Performance Concrete*, 2nd ed. John Wiley & Sons, Inc., 2001.

11. Balaguru P.N. and S.P. Shah, *Fiber-Reinforced Cement Composites*, NewYork: McGraw-Hill Inc., 1992.

12. Naaman A.E., "Fiber Reinforced Concrete: State of Progress at the Edge of the Millennium", *9th International Conference on Concrete Engineering and Technology*, Kuala Lumpur, Malaysia, pp. 20–48, 2006.

13. Brandt A.M., "Fiber Reinforced Cement-Based (FRC) Composites After Over 40 Years of Development in Building and Civil Engineering", *Composite Structures*, pp.3-9, 2008.

14. Lawler J.S., D. Zampini and S.P. Shah, "Permeability of Cracked Hybrid Fiber Reinforced Mortar Under Load", *ACI Materials Journal*, 99(4), pp. 379-385, 2002.

15. Banthia N., S. Mindess and J. Trottier, "Impact Resistance of Steel Fiber Reinforced Concrete", *ACI Materials Journal*, Vol. 93, No. 9, pp. 472-479, 1996

16. Naaman A.E. and S.P. Shah, "Pull-out Mechanism in Steel Fiber-Reinforced Concrete", *Journal of the Structural Division ASCE*, Vol. 102, No. ST8, pp. 1537–1548, 1976.

17. Valle M. And O. Buyukozturk, "Behavior of Fiber Reinforced High Strength Concrete Under Direct Shear", *ACI Materials Journal*, Vol. 90, No.2, pp. 122–133, 1994.

18. Chanh N.V., *Steel Fiber Reinforced Concrete*, Faculty of Civil Engineering, Ho Chi Minh City University of Technology.

19. Batson G., E. Jenkins and R. Spatney, "Steel Fibers as Shear Reinforcement in Beams", *ACI Journal*, Vol. 69, pp. 640–644, 1972.

20. Ferrara L. and A. Meda, "Relationships Between Fibre Distribution, Workability and the Mechanical Properties of SFRC Applied to Precast Roof Elements", *Materials and Structures*, Vol. 39, pp. 411–420, 2006.

21. Ferrara, L., N. Ozyurt and M. di Prisco, "High Mechanical Performance of Fiber-Reinforced Cementitious Composites: the Role of Casting Flow Induced Fiber Orientation", *Materials and Structures*, Accepted for publication, 2010.

22. Ferrara, L., Y.D. Park and S.P.Shah, "A Method for Mix-Design of Fiber-Reinforced Self-Compacting Concrete", *Cement and Concrete Research*, Vol. 37, No. 6, pp. 957-971, 2007.

23. Ferrara, L. and N. Ozyurt, "*Mix*-design Optimization of Steel Fiber Reinforced SCC", *2nd North American Conference on SCC*, Chicago, November, 2008.

24. Ozyurt, N., N. Tregger, L. Ferrara, I. Sanal and S.P. Shah, "Adapting Fresh State Properties of Fiber-Reinforced Cementitious Material for High Performance Thin-Section Elements", *3rd International Rilem Symposium on Rheology of Cement Suspensions such as Fresh Concrete*, pp. 313-321, Reykjavik, Iceland, 2009.

25. Shah, S.P., "Do Fibers Increase the Tensile Strength of Cement-Based Matrices?", *ACI Materials Journal*, Vol. 88, pp. 595-602, 1991.

26. Li, V.C., "Large Volume, High-Performance Applications of Fibers in Civil Engineering", *Journal of Applied Polymer Science*, Vol. 83, pp. 660-686, 2000.

27. Ferrara, L., A. Meda, T. Lamperti and F. Pasini, "Connecting Fiber Distribution, Workability and Mechanical Properties of SFRC: An Industrial Application to Precast Elements", *6th RILEM Symposium on Fibre-Reinforced Concretes*, Varenna, Italy, pp. 493-504, 2004.

28. Bentur, A., "Fiber-Reinforced Cementitious Materials", *Material Science of Concrete, The American Ceramic Society*, pp. 223-285, 1989.

29. Akkaya, Y., J. Picka and S.P. Shah, "Spatial Distribution of Aligned Short Fibers in Cement Composites", *Journal of Materials in Civil Engineering*, Vol. 12, pp. 272, 2000.

30. Chermant, J.L., L. Chermant, M. Coster, A.S. Dequiedt and C. Redon, "Some Fields of Applications of Automatic Image Analysis in Civil Engineering", *Cement and Concrete Composites*, Vol. 23, pp. 157-169, 2001.

31. Akkaya, Y., S.P. Shah and B. Ankenman, "Effect of Fiber Dispersion on Multiple Cracking of Cement Composites", Journal *of Engineering Materials in Civil Engineering*, Vol. 127, No. 4, pp. 311-316, 2001.

32. Chermant, J.L., L. Chermant, M. Coster, A.S. Dequiedt and C. Redon, "Some Fields of Applications of Automatic Image Analysis in Civil Engineering", *Cement and Concrete Composites*, Vol. 23, pp. 157-169, 2001.

33. Yang, Y., "Methods Study on Dispersion of Fibers in CFRC", *Cement and Concrete Research*, Vol. 32, pp. 747-750, 2002.

34. Akkaya, Y., J. Picka and S.P. Shah, "Spatial Distribution of Aligned Short Fibers in Cement Composites", *Journal of Materials in Civil Engineering*, Vol. 12, pp. 272, 2000.

35. Eberhardt, C., and A. Clarke, "Fiber-Orientation Measurements in Short-Glass-Fiber Composites. Part I: Automated, High Angular-Resolution Measurement by Confocal Microscopy," *Composites Science and Technology*, Vol. 61, pp. 1389-1400, 2001.

36. Edgington J. And D.J. Hannant, "Steel Fiber Reinforced Concrete: the Effect on Fiber Orientation of Compaction by Vibration", *Materiaux et Constructions*, Vol. 5, pp. 41-44, 1972.

37. Ozyurt, N., T.O. Mason and S.P. Shah, "Correlation of Fiber Dispersion, Rheology and Mechanical Performance of FRCs", *Cement and Concrete Composites*, Vol. 29, No. 2, pp. 70–79, 2007.

38. Schwartzentruber, L.D, R.L. Roy and J. Cordin, "Rheological Behaviour of Fresh Cement Pastes Formulated from a Self Compacting Concrete (SCC)", *Cement and Concrete Research*, Vol. 36, No. 7, pp. 1203-1213, 2006.

39. Ozyurt, N., *Connecting Fiber Dispersion, Rheology and Mechanical Performance for Fiber Reinforced Cement Based Materials*, PhD Thesis, Istanbul Technical Institute, 2005.

40. CEN – *European Committee for Standardization. Steel Fibre Reinforced Concrete Definitions, Classification and Designation*. UNI 11039-1, 2003.

41. ACI Committee 544, "Guide for Specifying, Mixing, Placing and Finishing Steel Fiber Reinforced Concrete", *ACI Materials Journal*, Vol. 90, No. 1, pp. 94-101, 1993.

42. Nataraja, M.C., N. Dhang and A.P. Gupta, "Toughness Characterization of Steel Fiber-Reinforced Concrete by JSCE Approach", *Cement and Concrete Research*, Vol. 30, pp.593-597, 2000.

43. Soroushian, P. and Z. Bayasi, “Fiber Type Effects on the Performance of Steel Fiber Reinforced Concrete”, *ACI Materials Journal*, Vol. 88, No.2, pp. 129-134, 1991.

44. Chen,L., S. Mindess and D.R. Morgan, “Specimen Geometry and Toughness of Steel Fiber Reinforced Concrete”, *ASCE Journal of Materials and Civil Engineering*, Vol. 6, No. 4, pp. 529- 541, 1994.

45. ASTM-American Standard of Testing Materials, *Standard Test Method for Flexural Performance of Fiber-Reinforced Concrete (Using Beam With Third-Point Loading)*, ASTM C1609/1609M, 2010.

46. Boulekbache, B., M. Hamrat, M. Chemrouk and S. Amziane, “Flowability of Fibre-Reinforced Concrete and Its Effect on the Mechanical Properties of the Material”, *Journal of Construction and Building Materials*, Vol. 24, pp. 1664-1671, 2010.

47. Lianrong, C., *Flexural Toughness of Fibre Reinforced Concrete*, Graduate Thesis, University of British Columbia, 2009.

48. Advani, S.G., and C.L. Tucker, “The Use of Tensors to Describe and Predict Fiber Orientation in Short Fiber Composites”, *Journal of Rheology*, Vol. 31, No. 8, pp.751-784, 1987.

49. Yazici, S., G. Inan and V. Tabak, “Effect of Aspect Ratio and Volume Fraction of Steel Fiber on the Mechanical Properties of SFRC”, *Construction and Building Materials*, Vol. 21, pp. 1250–1253, 2007.

50. Ozyurt, N., A. Ilki, C. Tasdemir, M.A. Tasdemir and M. Yerlikaya, “Mechanical Behavior of High Strength Steel Fiber Reinforced Concretes with Various Steel Fiber Content”s, *5th International Congress on Advances in Civil Engineering*, Istanbul, Turkey, pp. 885-894, September, 2002.

51. Taylor, M., F.D. Lydon and B.I.G. Barr, “Toughness Measurements on Steel Fibre-Reinforced High Strength Concrete”, *Cement and Concrete Composites*, Vol. 19, pp. 329–340, 1997.

52. ACI Committee 544, “Measurement of Properties of Fiber Reinforced Concrete”, *ACI Materials Journal*, *Vol.* 85, No. 6, pp. 583-589, 1988.